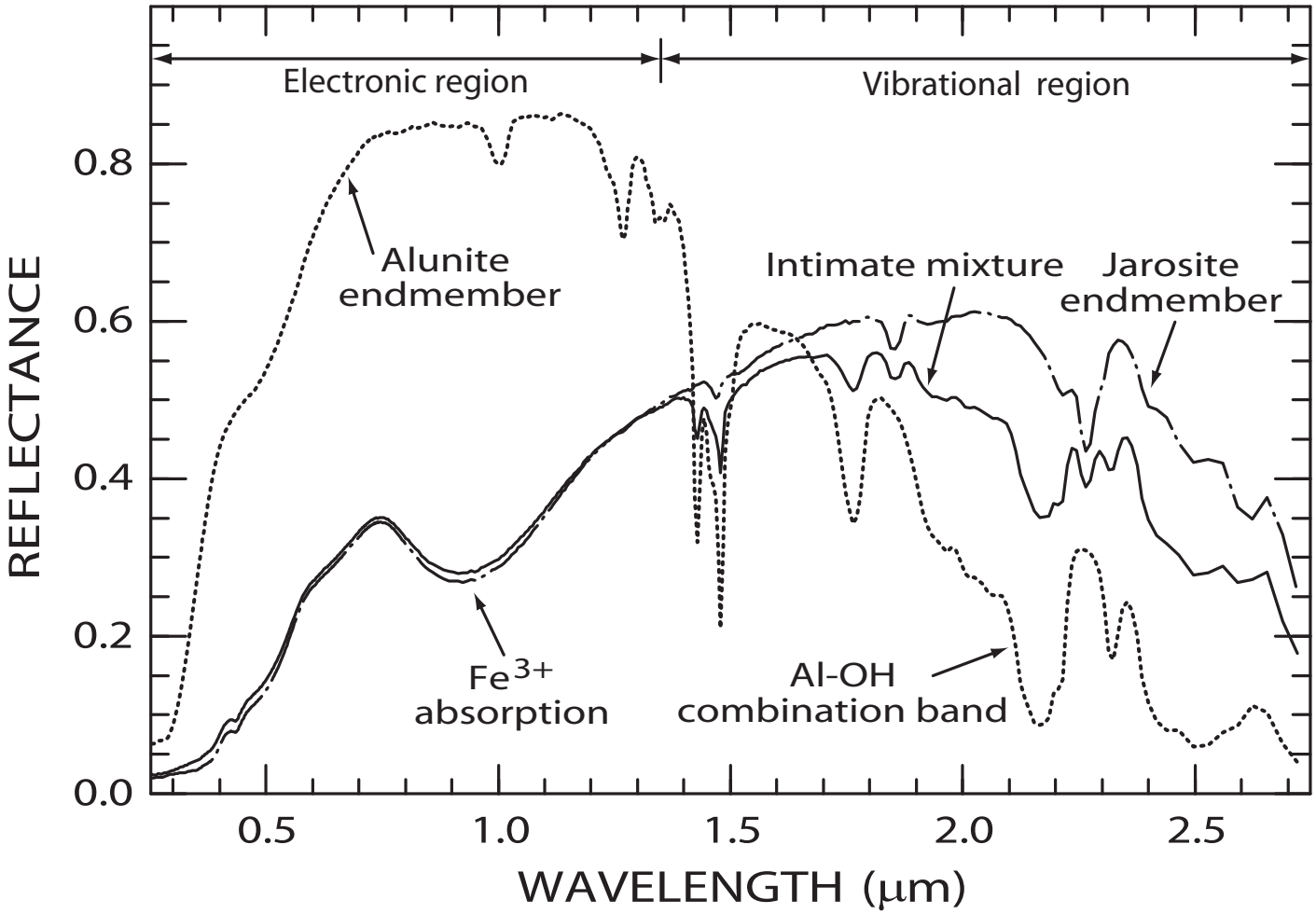

Figure 1. Reflectance spectra of an intimate mixture of 50 wt% alunite and 50 wt% jarosite, as well as alunite and jarosite endmembers. Jarosite has an electronic Fe^{3+} absorption at 0.95 μm and alunite has a vibrational Al-OH combination absorption band at 2.17μm. Note that jarosite spectrally dominates the electronic region while alunite dominates the vibrational region in the intimate mixture.

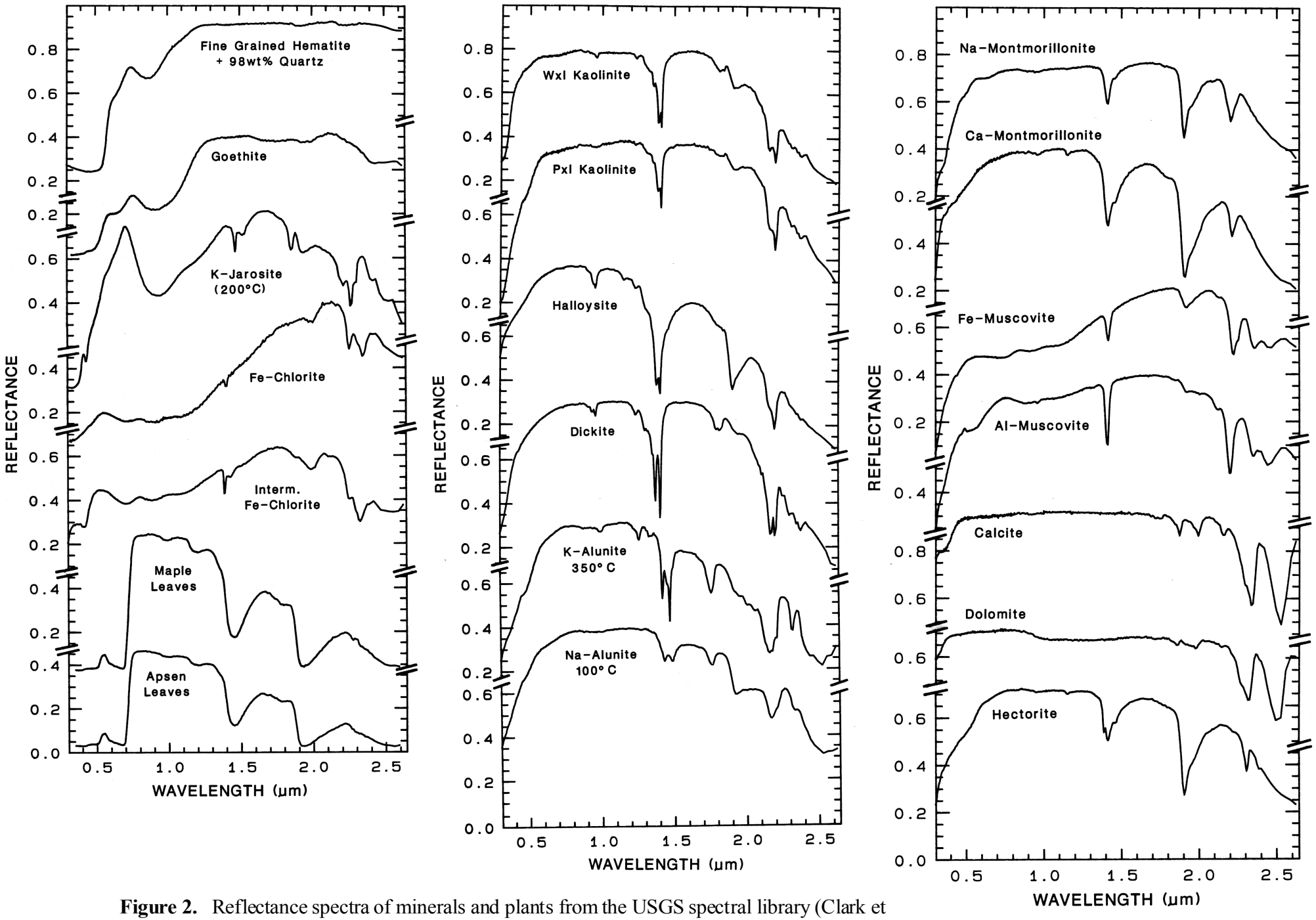

Figure 2. Reflectance spectra of minerals and plants from the USGS spectral library (Clark et al., 1993a). Interm. = intermediate; Wxl = well-crystallized; Pxl = poorly-crystallized.

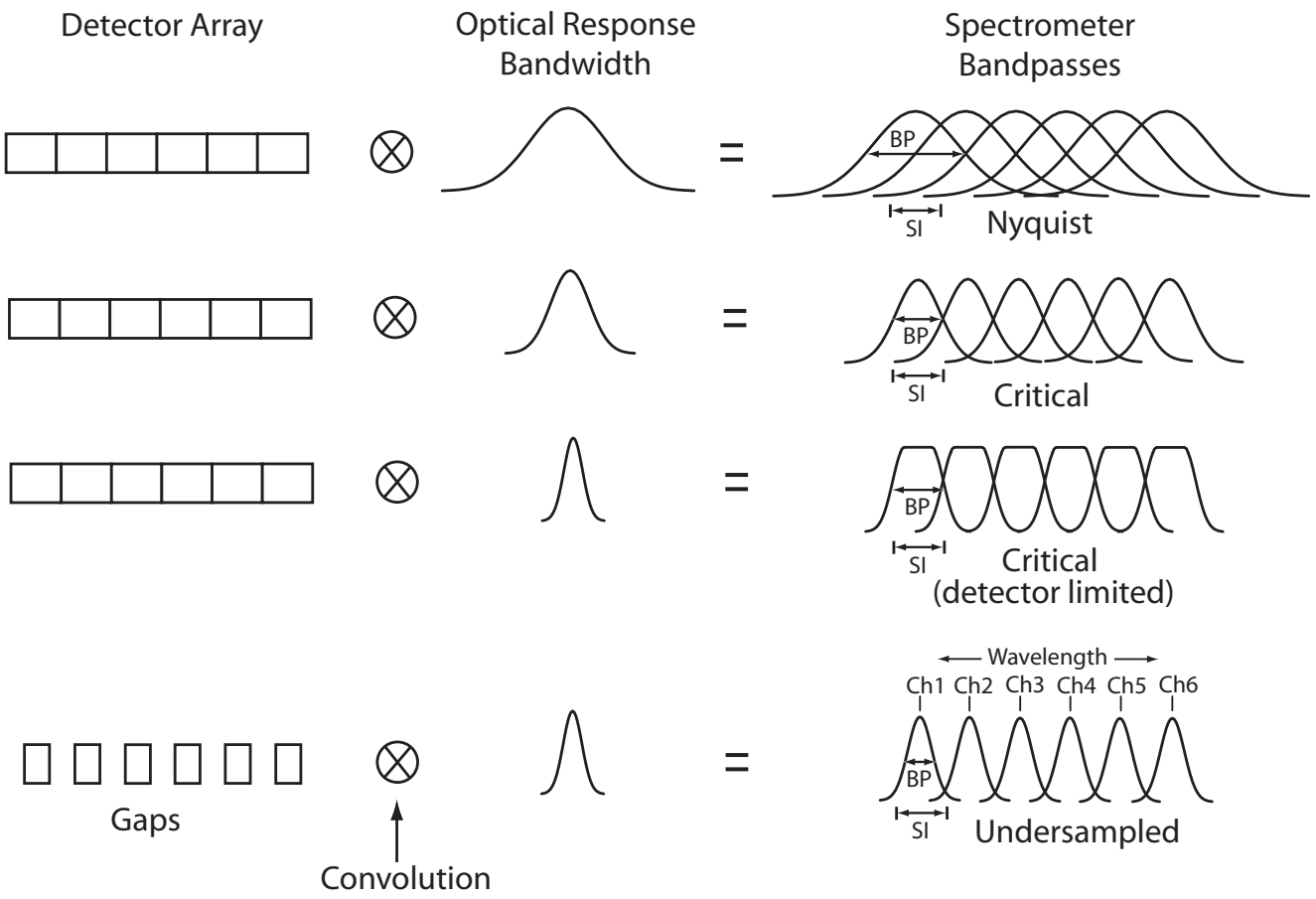

Figure 3. Definition of different types of spectral sampling in spectrometers. Nyquist sampling occurs when the bandpass (BP) is twice the sampling interval (SI). Critical sampling occurs when the BP and the SI are comparable. Detector limited critical sampling occurs when the optical response bandwidth is narrower than the spectral width of the detectors resulting in flat topped bandpasses. Undersampling occurs when the BP is less then the SI. The implication in undersampling is that light is being wasted between adjacent spectral channels. The spectrometer BP is the convolution of the optical response bandwidth and the spectral width of a detector.

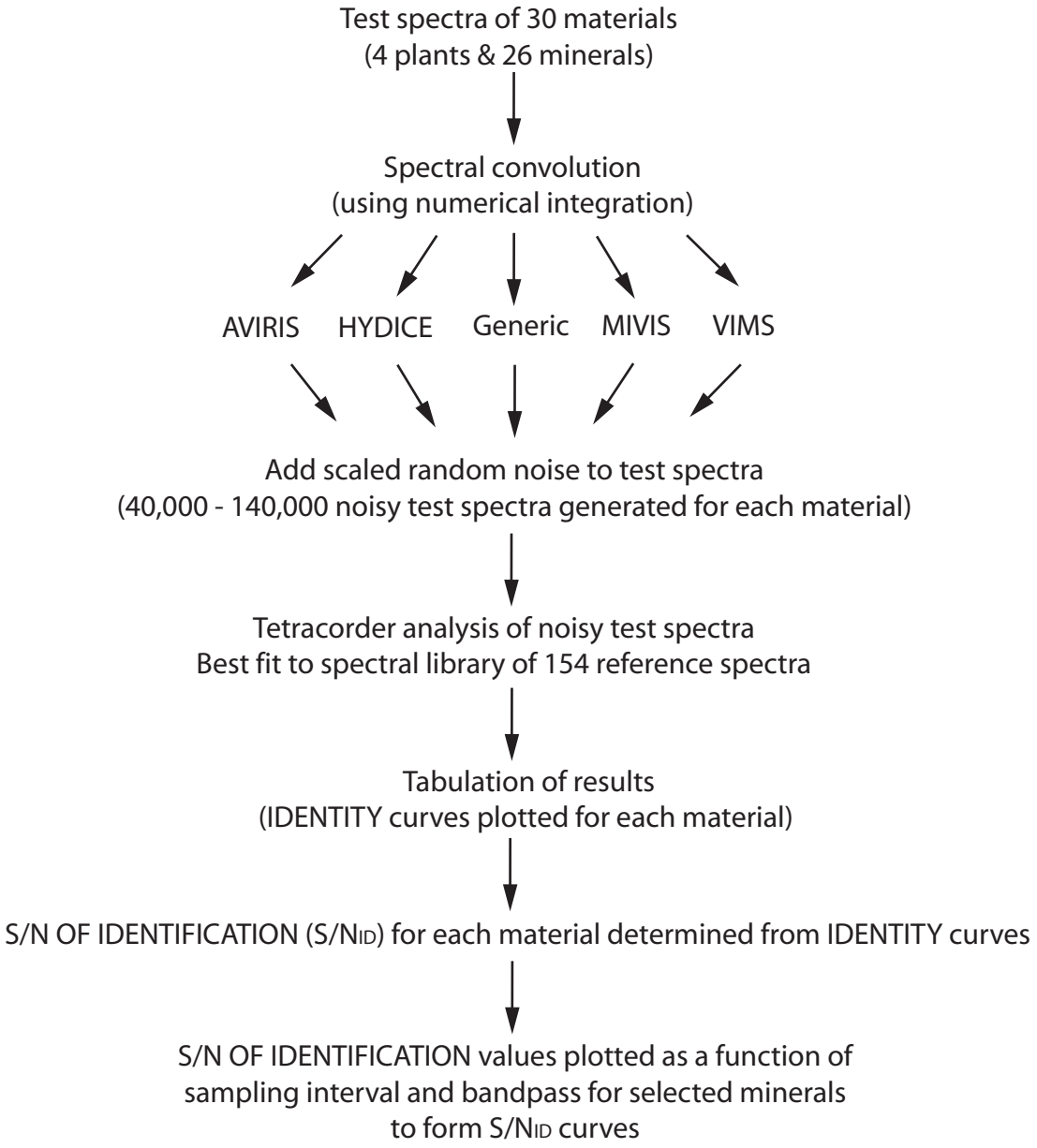

Figure 4. Steps involved in processing and spectral identification of test spectra to derive spectral identity curves and signal-to-noise of identification values.

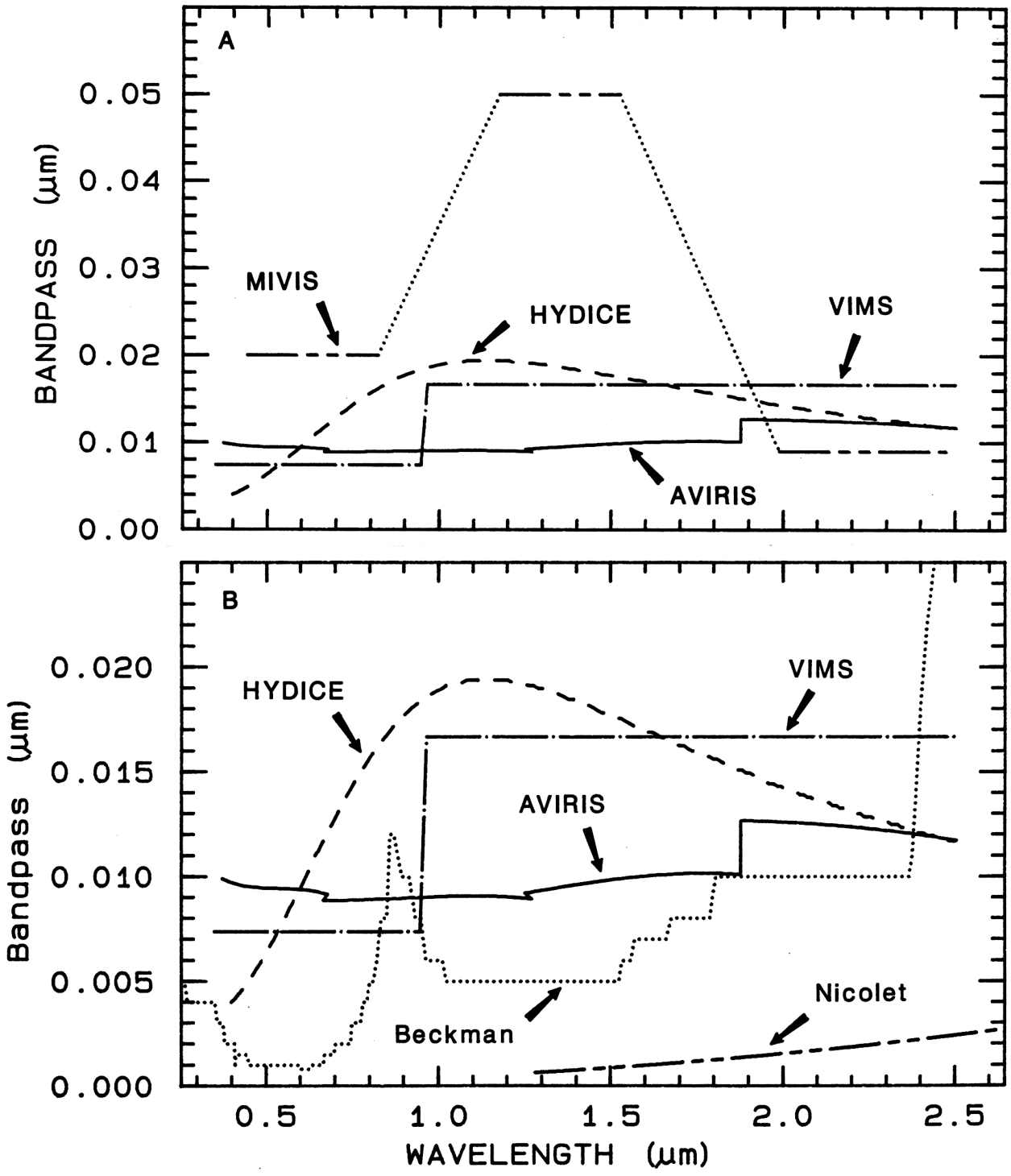

Figure 5. A) Spectral bandpasses of the AVIRIS, HYDICE, VIMS and MIVIS imaging spectrometers. All spectrometers except MIVIS have continuous spectral coverage from 0.4-2.5 μm (VIMS covers the range from 0.3-5.1 μm). MIVIS has no spectral coverage between 0.83-1.15 and 1.55-2.00 μm (gaps shown as dotted lines) but does have additional coverage from 8.2-12.7 μm which was not simulated in this study. B) Imaging spectrometer bandpasses compared to USGS Spectroscopy Laboratory Beckman and Nicolet spectrometer bandpasses.

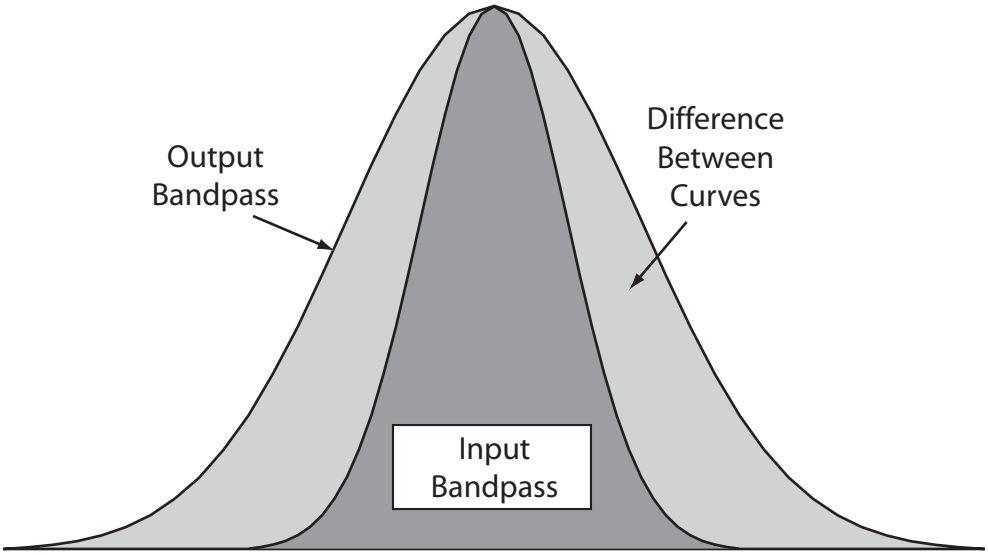

Figure 6. During spectral convolution the difference in area between input and output spectrometer bandpasses is represented by the integrals in Equation 2.

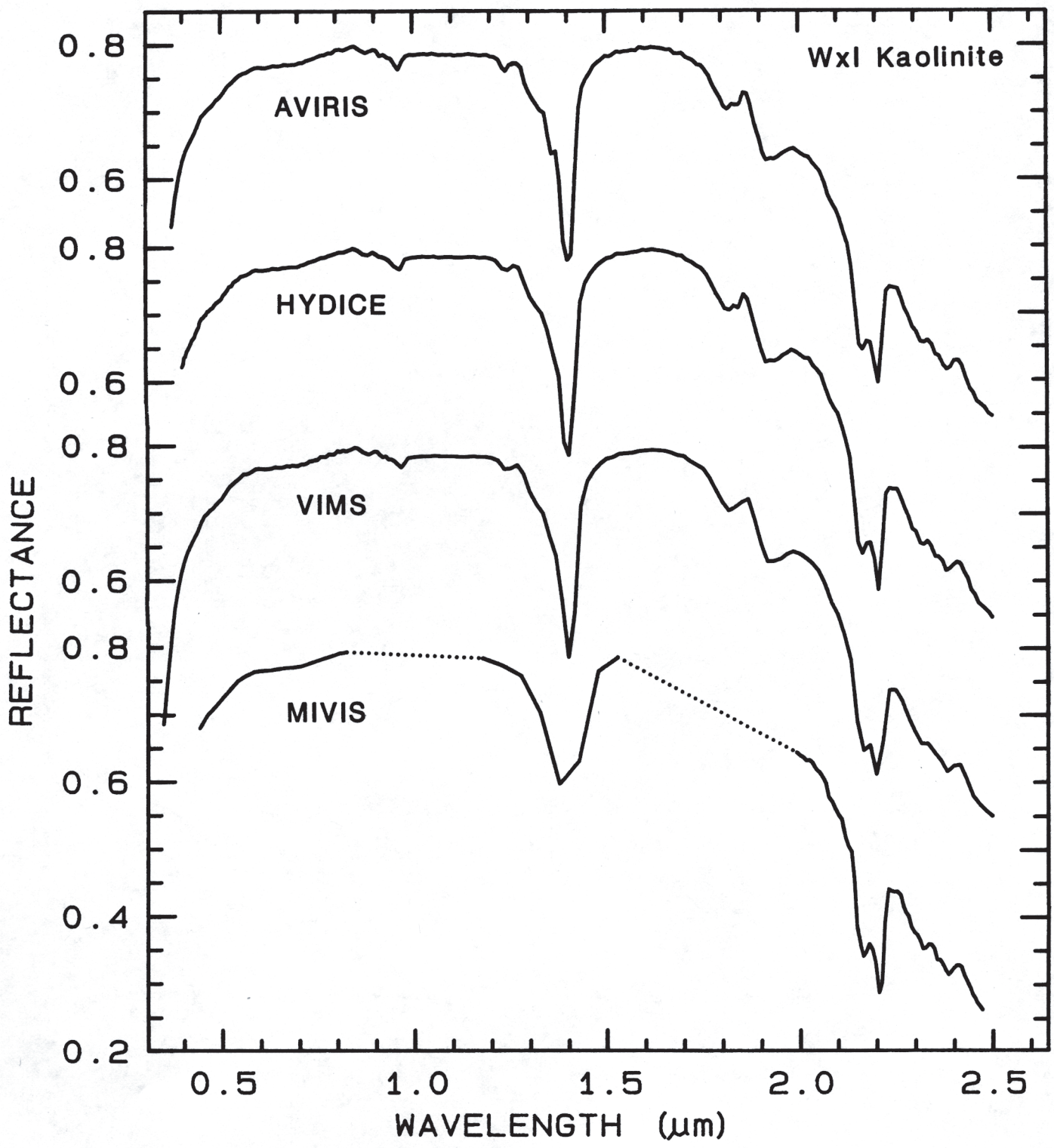

Figure 7. Reflectance spectra of a well-crystallized kaolinite convolved to AVIRIS, HYDICE, VIMS, and MIVIS resolution. Dotted lines in the bottom spectrum represent wavelengths regions where spectral data is not collected by the MIVIS instrument.

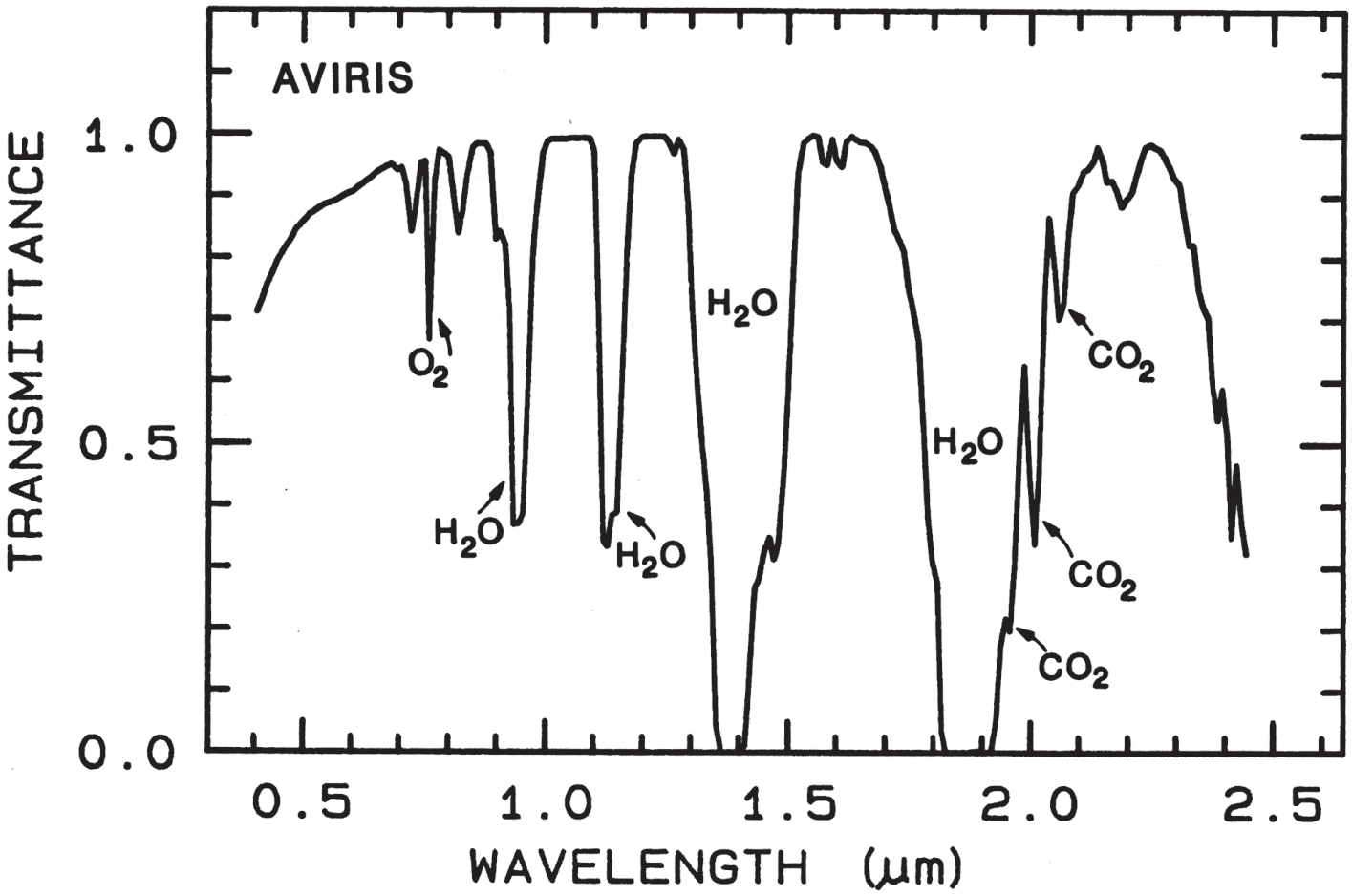

Figure 8. Transmission spectrum of the Earth's atmosphere at AVIRIS resolution calculated using the LOWTRAN atmospheric modeling program (Kneizys et al., 1989). Model uses a single path (top of atmosphere to surface) with mid-latitude summer sun and atmospheric conditions. Terrestrial atmospheric H_2O absorptions are frequently strong enough to conceal surface absorptions at 1.4 and 1.9 μm preventing these spectral regions from being used to map materials at the surface.

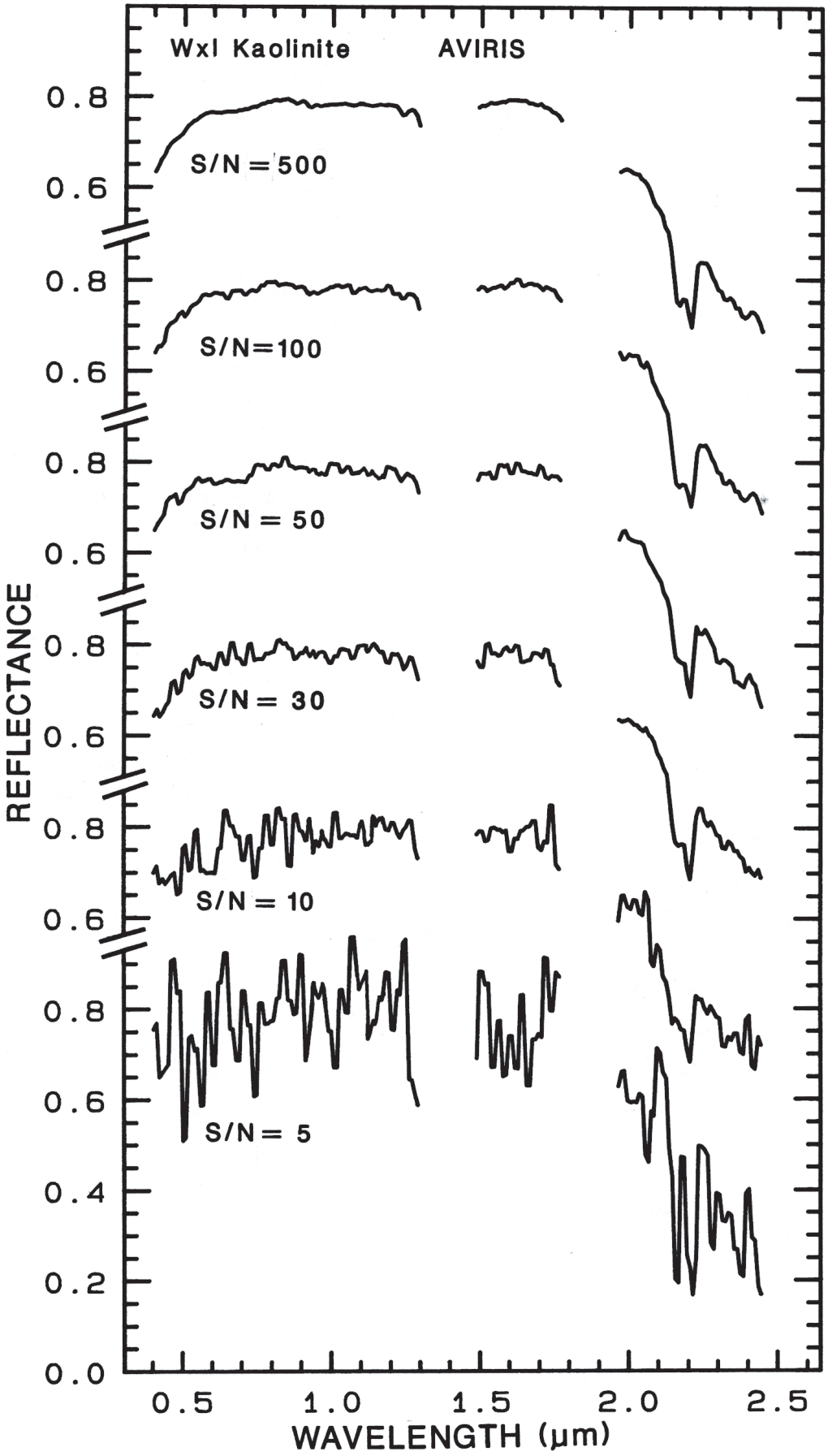

Figure 9. Laboratory spectrum of kaolinite convolved to AVIRIS resolution with various levels of random noise added. Signal-to-noise ratio is defined here as fifty percent reflectance divided by the standard deviation of the Gaussian noise, with the standard deviation of the noise at a constant level at all wavelengths over the entire spectrum.

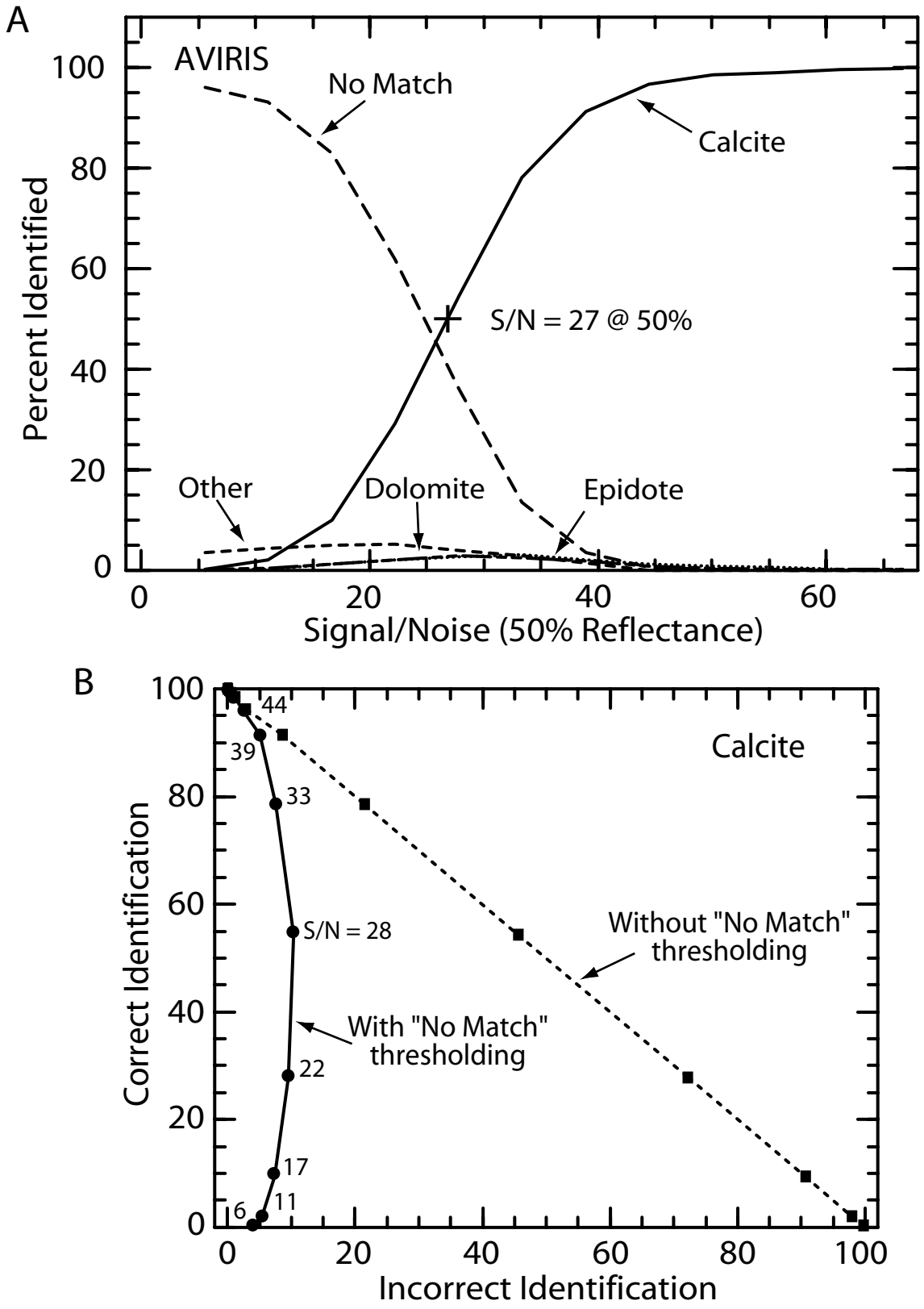

Figure 10. A) Percentage of noisy calcite test spectra correctly identified by Tetracorder as a function of signal-to-noise ratio (S/N) at AVIRIS spectral resolution. This is the calcite identity curve. The curves labeled dolomite and epidote give the percentage of noisy calcite spectra misidentified as those of dolomite and epidote respectively. "Other" refers to the percentage of spectra misidentified as those of materials other than dolomite and epidote. "No Match" refers to the percentage of spectra with Fit, Depth, or Fit*Depth values which fell below Tetracorder thresholds. Fifty percent of the noisy test spectra were correctly identified as calcite at a S/N of 27. The S/N values are for a 50% reflectance surface. B) Receiver operating characteristic curve for noisy calcite test spectra. Numbers next to circles are the S/N values of the test spectra and also apply to the corresponding squares. Most test spectra are incorrectly identified at low S/N (dashed curve) but with the "No Match" threshold activated (solid curve) the number of test spectra incorrectly identified decreases substantially.

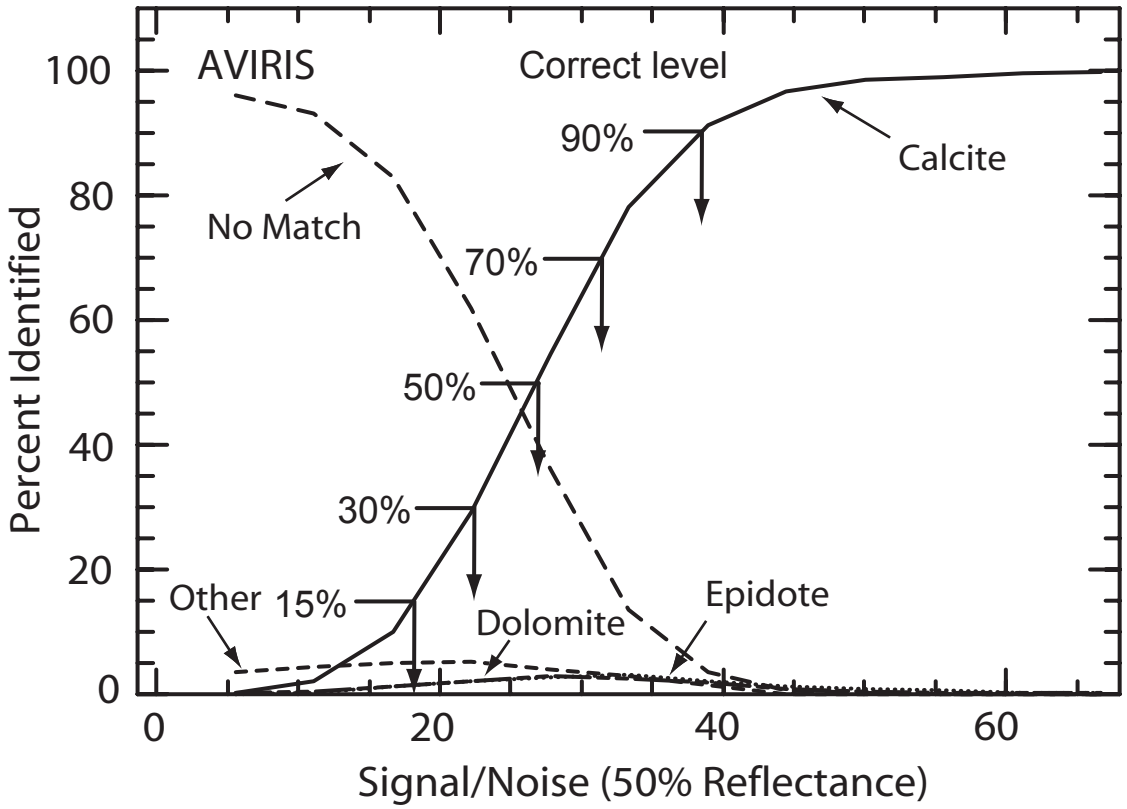

Figure 11. Identity curve for calcite at AVIRIS spectral resolution (Figure 10A). Arrows indicate the signal-to-noise of identification (S/N_{ID}) values (on the Signal / Noise axis) at the 15, 30, 50, 70, and 90% correct levels. The proportion of calcite, dolomite, epidote, "Other", and "No Match" identifications can be calculated for each S/N_{ID} value using this diagram.

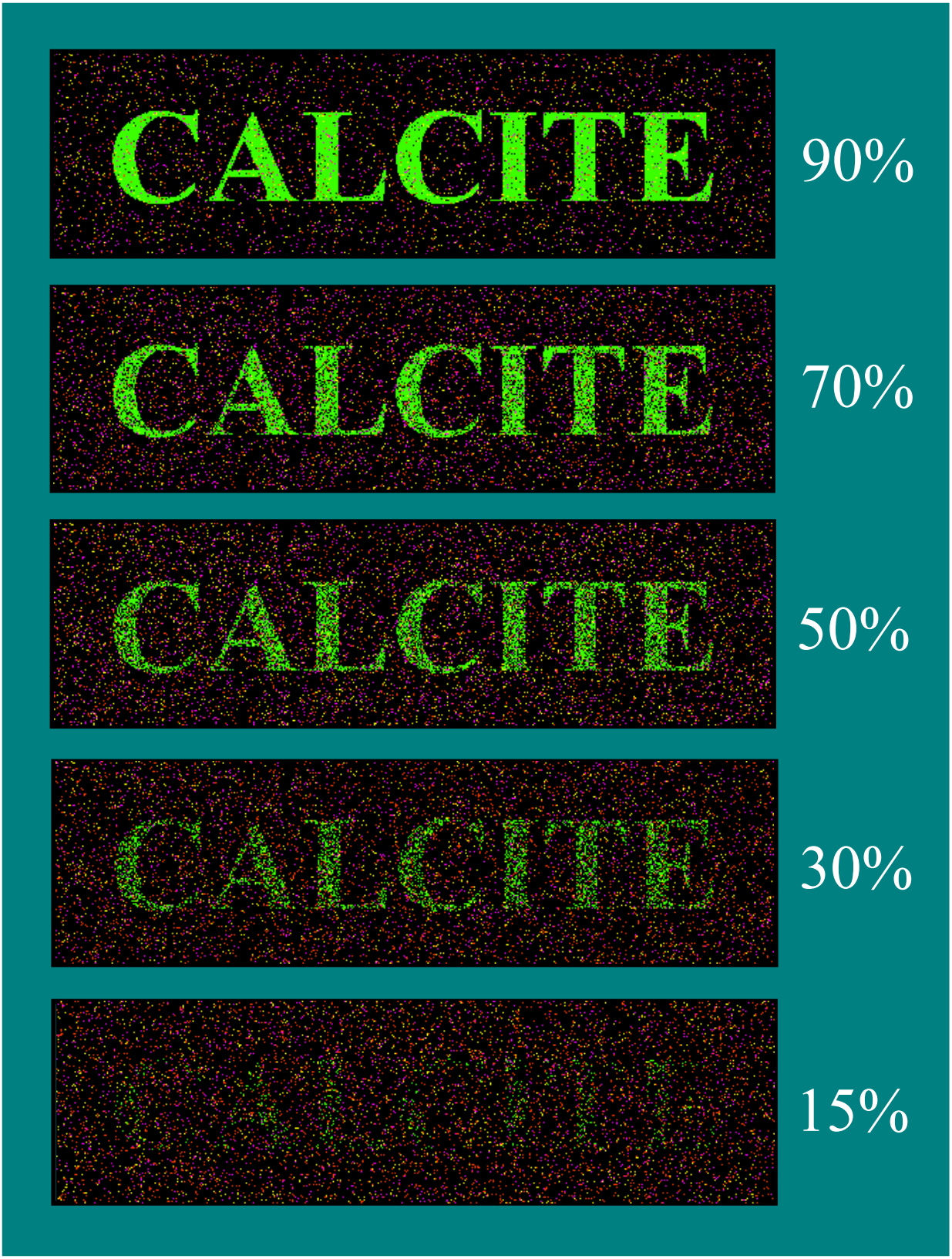

Figure 12. Synthetic color composite images based on the spectral identity curve for calcite (Figure 11) showing the effects of signal-to-noise ratio on the ability to correctly identify materials and recognize distribution patterns. The percentage of colored pixels in each image correspond to the proportion of calcite (green), dolomite (yellow), epidote (magenta), "Other" (red), and "No Match" (black) identified by Tetracorder using noisy calcite test spectra at the 15, 30, 50, 70, and 90 % correct levels. To create a cluster of pixels (e.g., a pattern similar to a geologic outcrop) as would be seen in noisy imaging spectrometer data all green calcite pixels were made black except in the letters of the word "calcite."

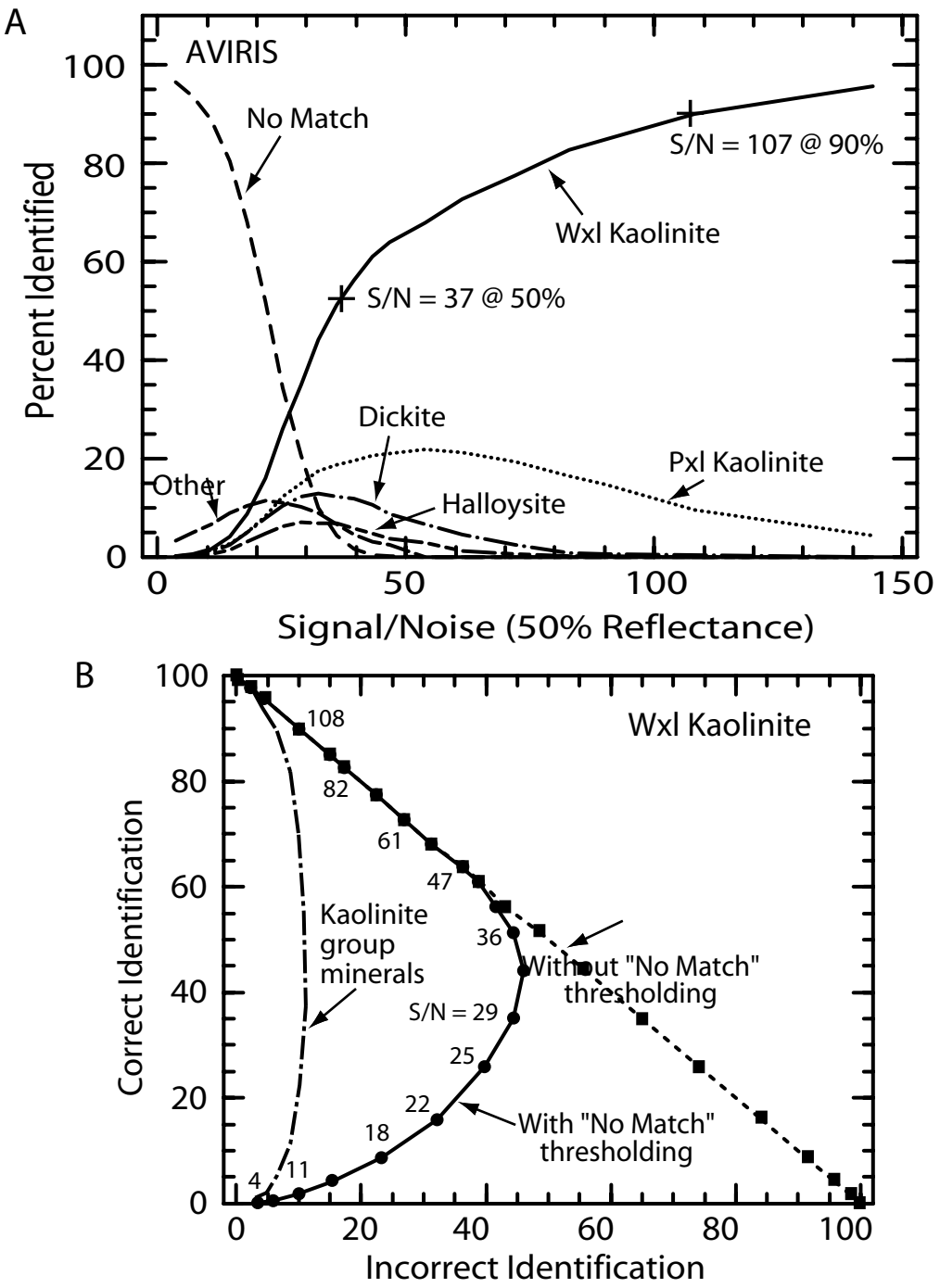

Figure 13. A) Percentage of noisy well-crystallized (wxl) kaolinite test spectra correctly identified by Tetracorder as a function of signal-to-noise ratio (S/N) at AVIRIS spectral resolution. This is the wxl kaolinite identity curve. The curves labeled dickite, halloysite, and poorly-crystallized (pxl) kaolinite give the percentage of spectra misidentified as those minerals. "Other" refers to the percentage of spectra misidentified as those of materials other than dickite, halloysite, and pxl kaolinite. "No Match" refers to the percentage of spectra with Fit, Depth, or Fit*Depth values which fell below Tetracorder thresholds. The other three spectrometers have similar curves. Fifty percent of the noisy kaolinite test spectra were correctly identified by Tetracorder at a S/N of 37; ninety percent were correctly identified at a S/N of 107. B) Receiver operating characteristic curve for noisy wxl kaolinite test spectra. Numbers next to circles are the S/N values of the test spectra and also apply to the corresponding squares. Most test spectra are incorrectly identified at low S/N (dashed curve) but with the "No Match" threshold activated (solid curve) the number of test spectra incorrectly identified decreases substantially. Dash-dot curve lumps the other kaolinite group minerals (e.g. pxl kaolinite, dickite, and halloysite) with wxl kaolinite to show that most of the incorrect identifications are due to confusion with these spectrally similar minerals.

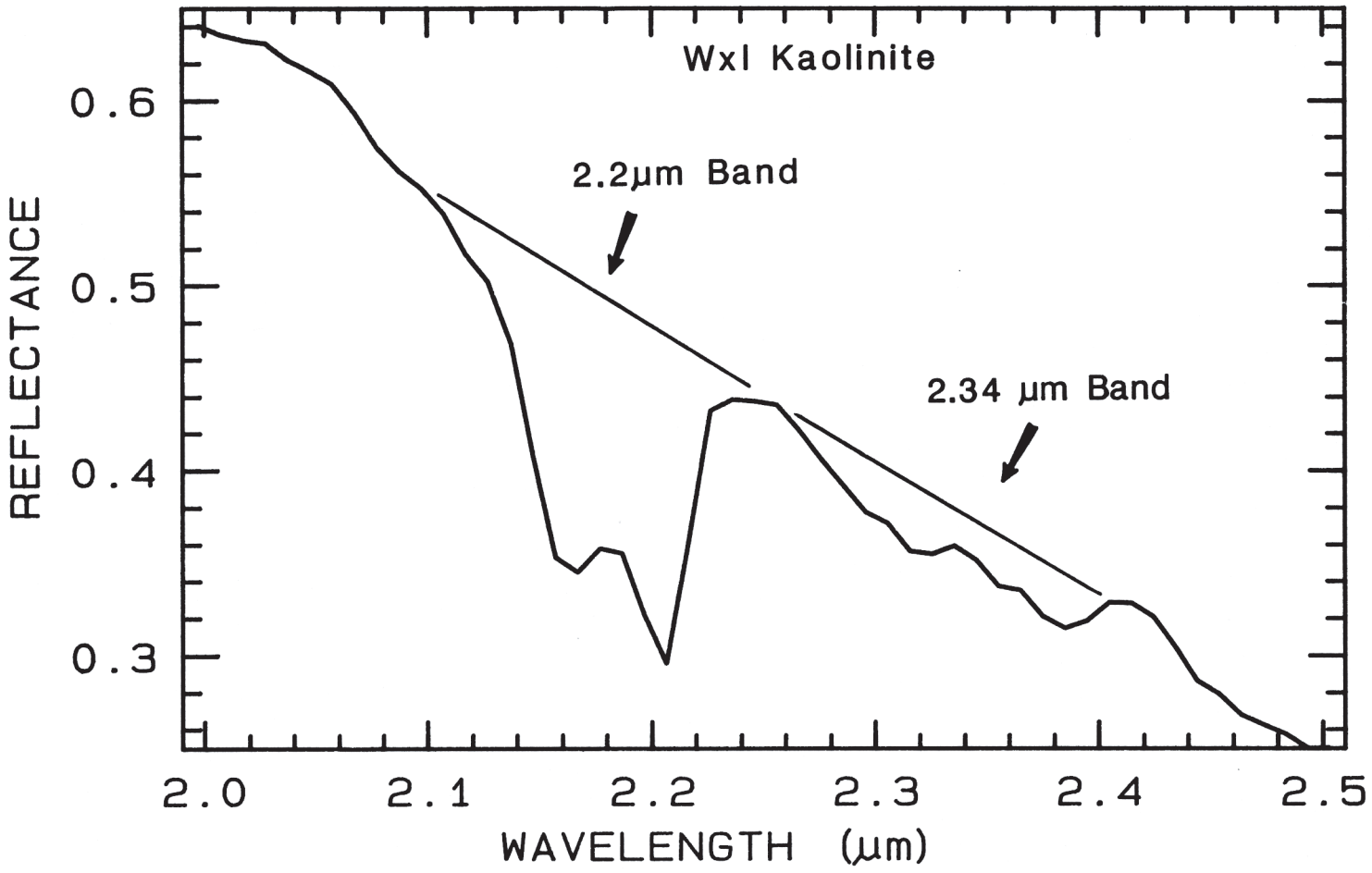

Figure 14. Reflectance spectrum of well-crystallized kaolinite showing details of the 2.2- and 2.34-µm absorptions and their continua.

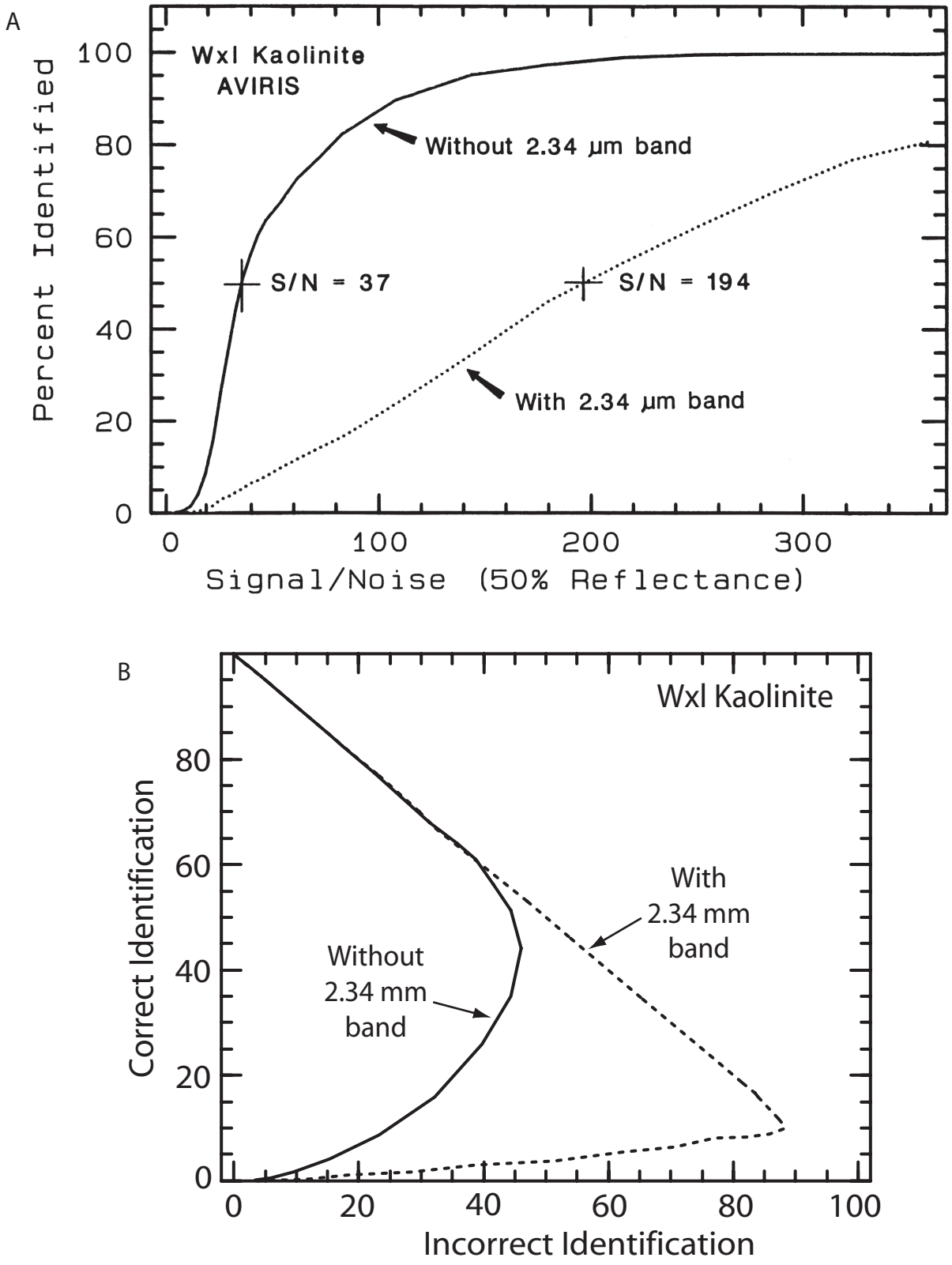

Figure 15. A) Identity curves for well-crystallized kaolinite at AVIRIS spectral resolution with and without inclusion of the 2.34-µm subordinate absorption in the Tetracorder analyses. Note the signal-to-noise ratio required for 50% correct identification of noisy kaolinite test spectra, using the 2.34- and 2.2-µm absorptions, is significantly higher than that required using only the 2.2-µm doublet for identification. B) Receiver operating characteristic curves for well-crystallized kaolinite with and without inclusion of the 2.34-µm subordinate absorption in the Tetracorder analyses.

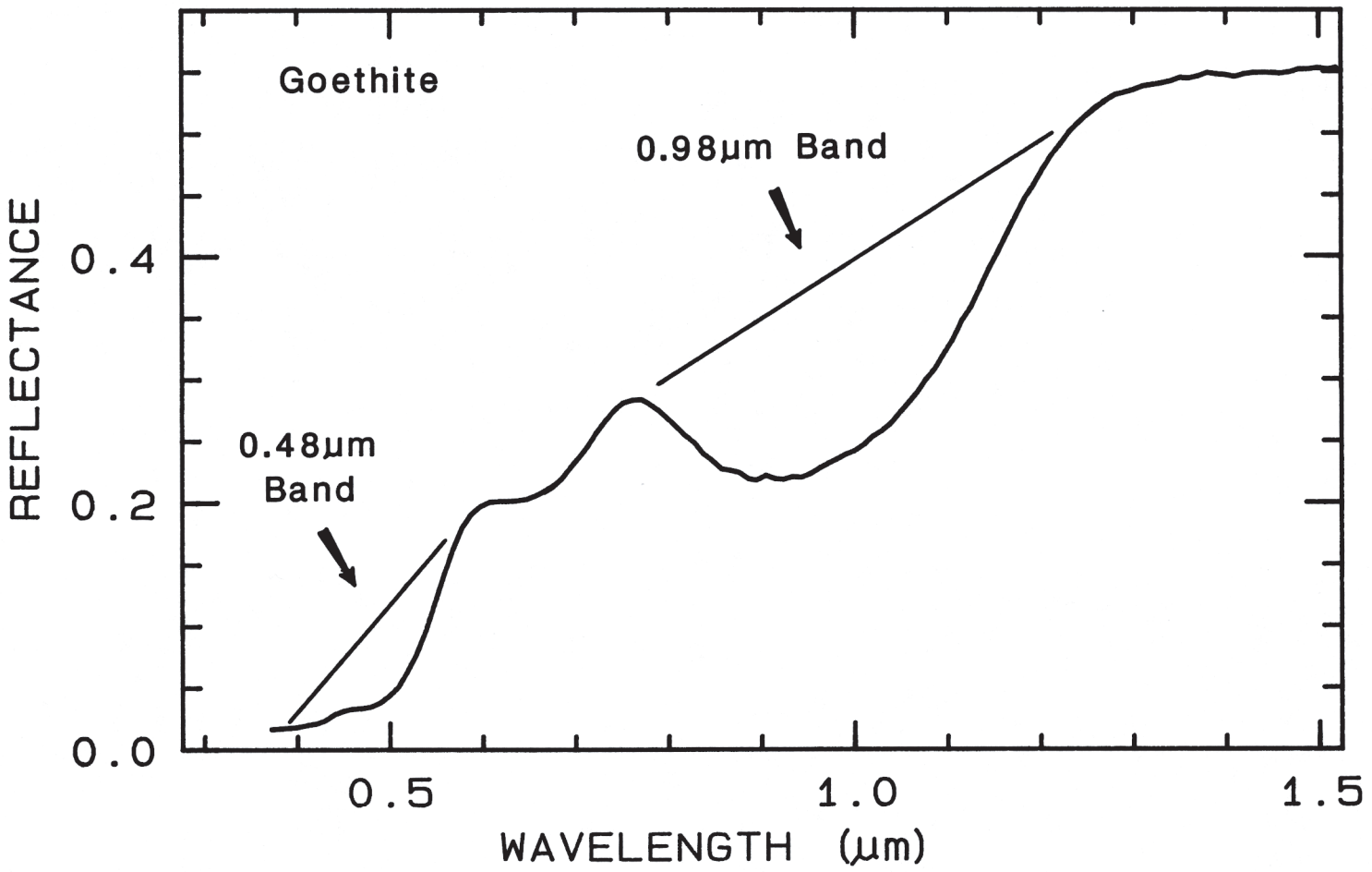

Figure 16. A reflectance spectrum of goethite with continua over the diagnostic absorption bands.

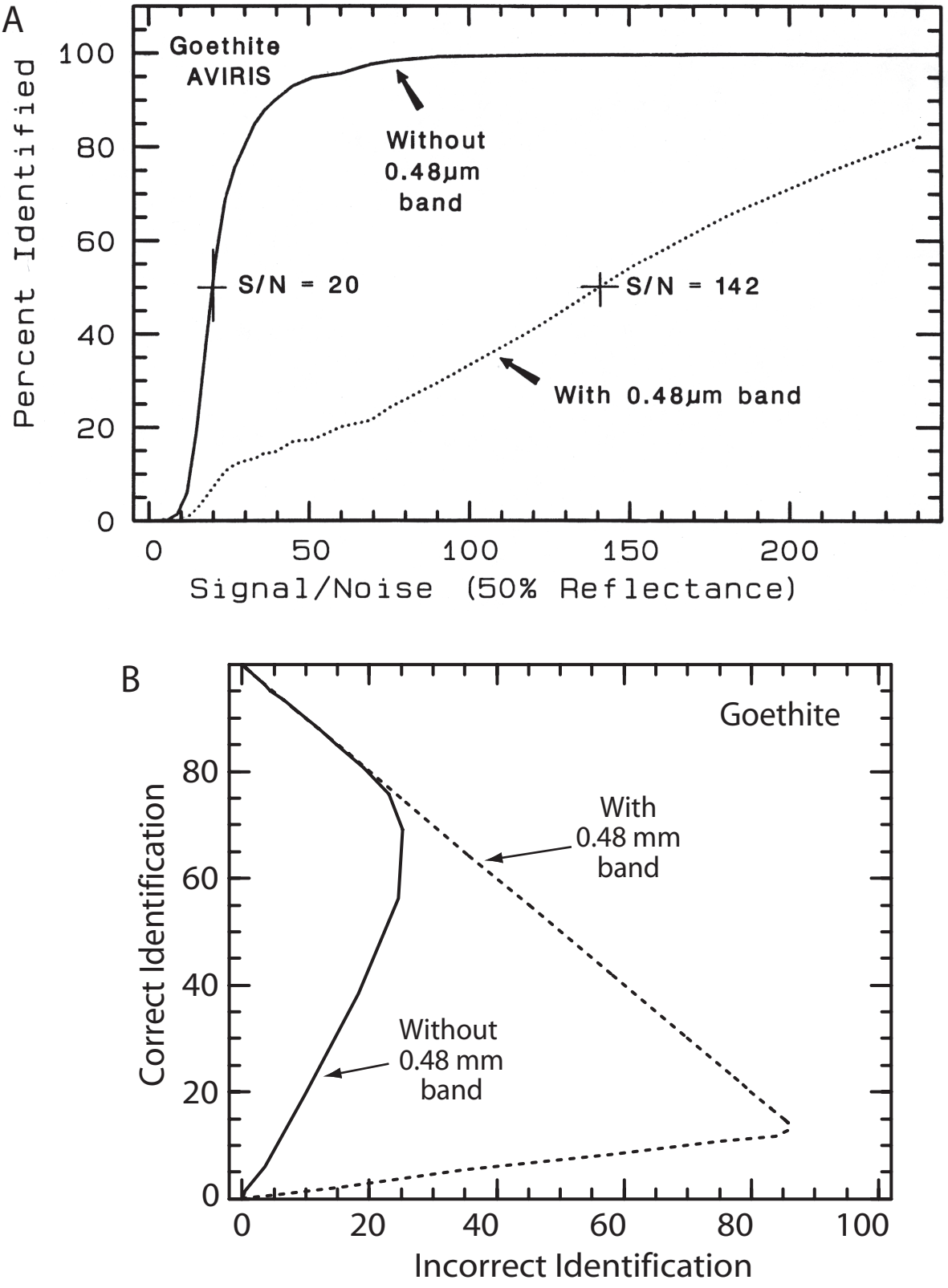

Figure 17. A) Goethite identity curves at AVIRIS spectral resolution with and without the use of the 0.48-µm absorption in Fit calculations. Because the 0.48-µm absorption is spectrally saturated, giving it a low reflectance, addition of random noise, uniform in magnitude at all wavelengths, preferentially degrades the Fit Tetracorder derived for goethite. B) Receiver operating characteristic curves with and without the use of the goethite 0.48-µm absorption in Fit calculations.

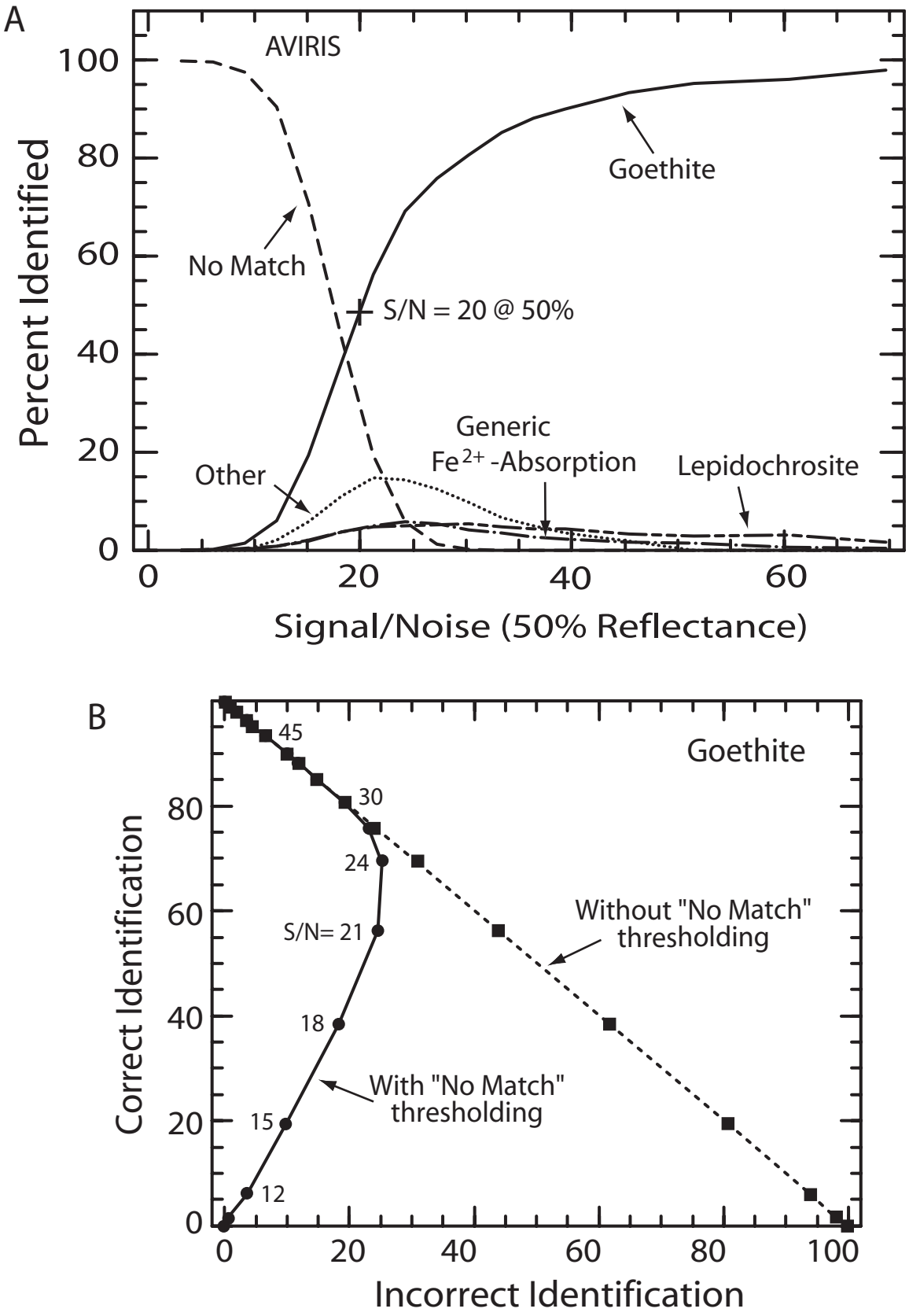

Figures 18. A) Percentage of noisy goethite test spectra correctly identified by Tetracorder as a function of signal-to-noise ratio (S/N) at AVIRIS spectral resolution using only the 0.98-μm absorption for Fit calculations. See text for explanation of curves. B) Receiver operating characteristic curves for noisy goethite test spectra. Numbers next to circles are the S/N values of the test spectra and also apply to the corresponding squares. Most test spectra are incorrectly identified at low S/N (dashed curve) but with the "No Match" threshold activated (solid curve) the number of test spectra incorrectly identified decreases substantially.

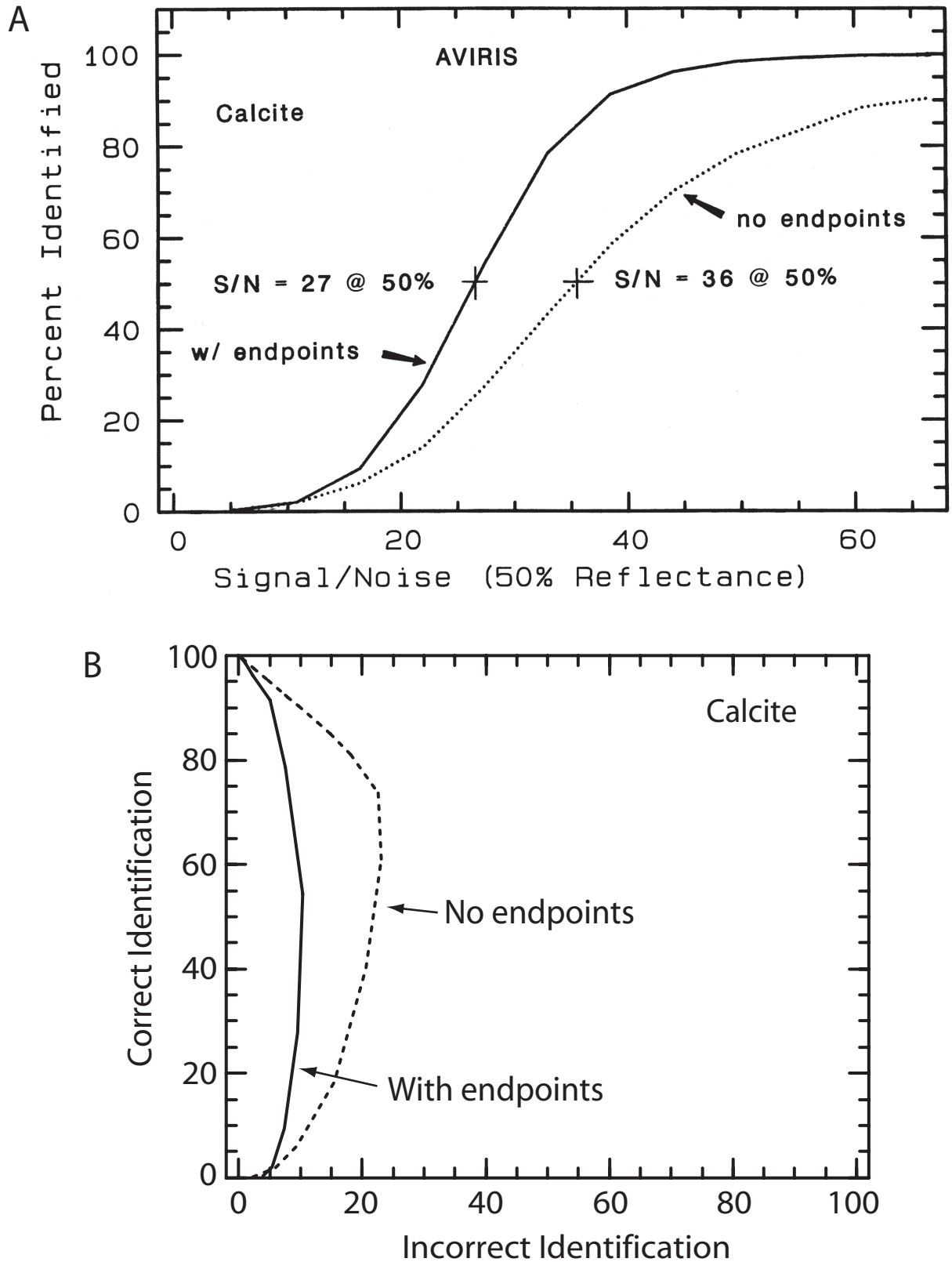

Figure 19. A) Identity curves for calcite at AVIRIS spectral resolution with and without the use of continuum endpoints in the Fit calculations. In general, for a given level of signal-to-noise ratio use of continuum endpoints increases the accuracy of Tetracorder identifications by25% for calcite and up to 50% for other minerals. B)Receiver operating characteristic curves for identification of noisy calcite spectra with and without the use of continuum endpoints in the Fit calculations.

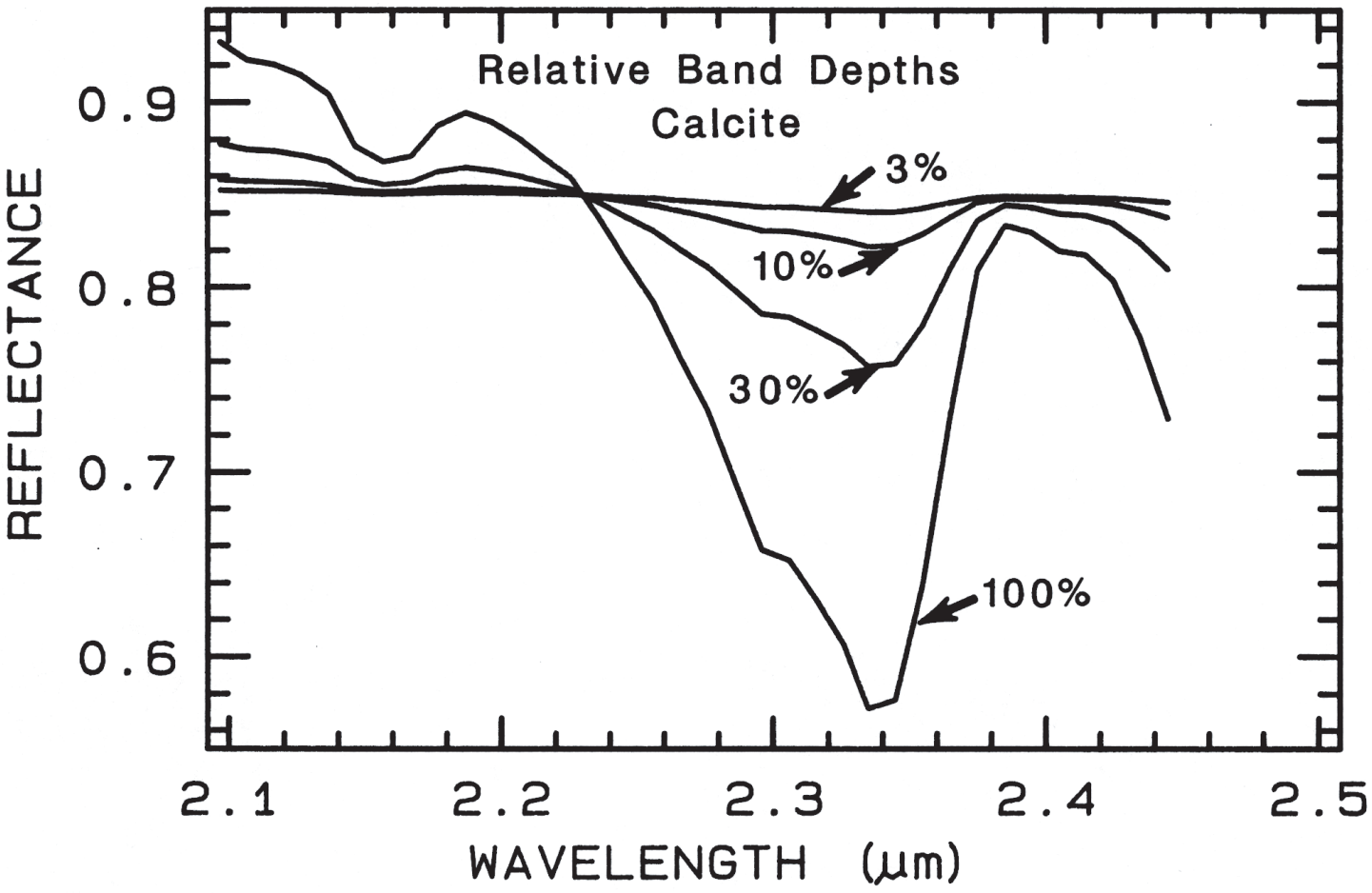

Figure 20. Reflectance spectra of the calcite 2.34-μm absorption at different band depths. All spectra were produced from the 100% strength absorption by multiplying by the appropriate fraction and adding a constant to restore the spectrum to its original reflectance level. This series of spectra simulate areal mixtures of calcite with a spectrally bland material in proportions that reduce the 2.34-μm absorption depth to the indicated level.

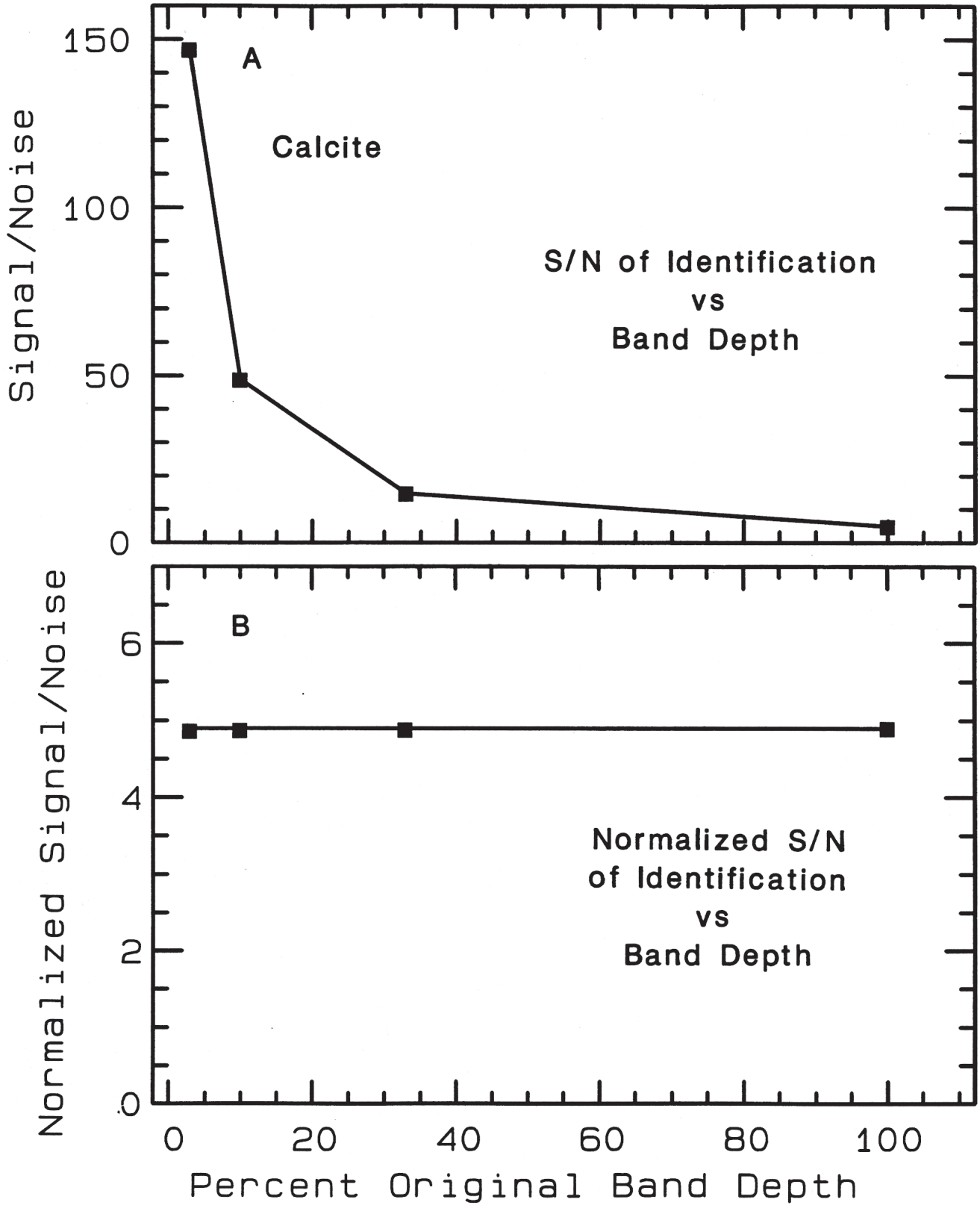

Figure 21. A) Signal-to-noise of identificationat 50% correct level as a function of the percentage of the original band depth for the calcite spectra shown in Figure 20. B) Signal-to-noise of identification (S/N_{ID}) normalized by dividing by the percent original band depth. Because these values plot on a horizontal line, the S/N_{ID} increases linearly as band depth decreases.

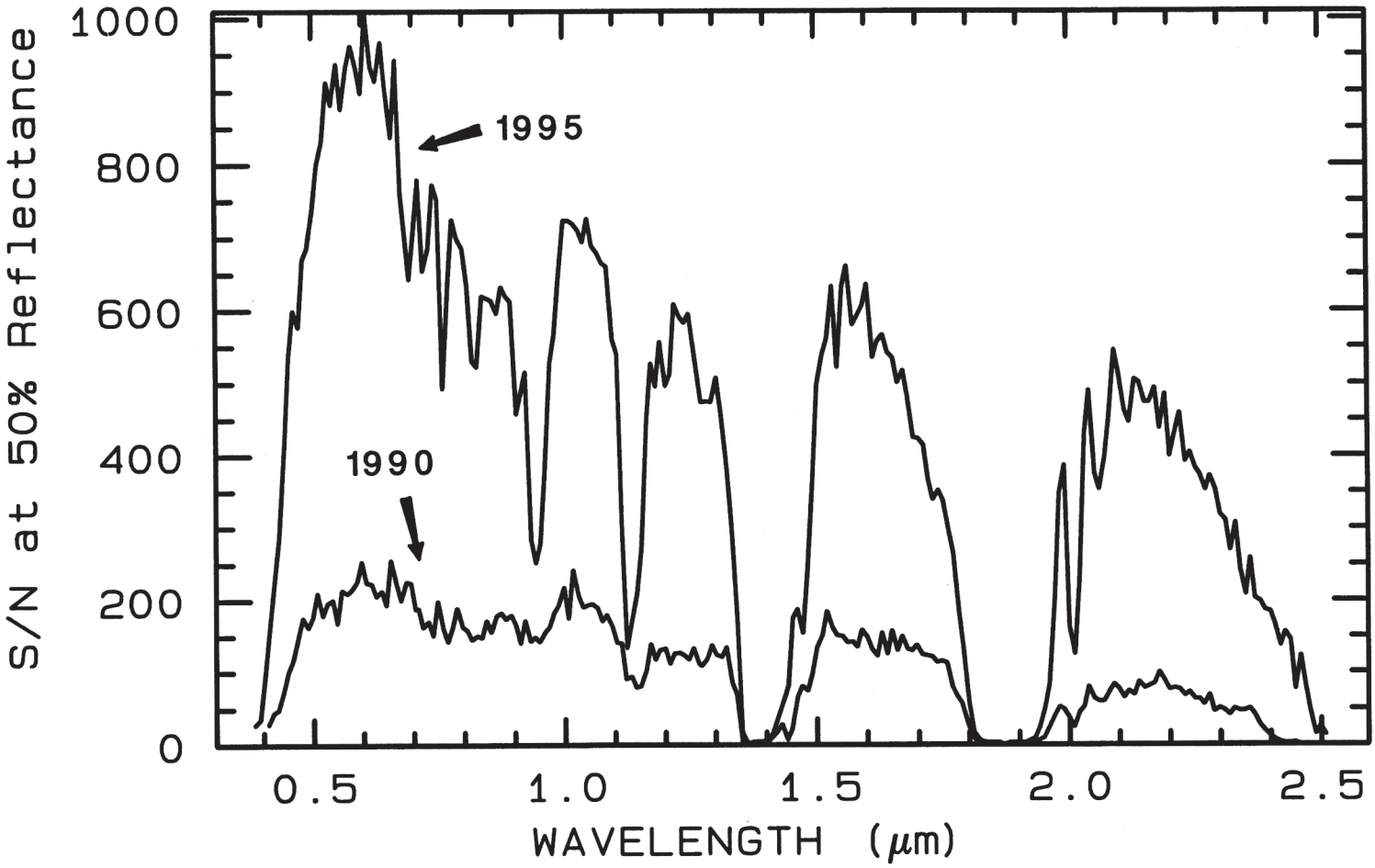

Figure 22. Signal-to-noise ratios (S/N) at 50% reflectance of AVIRIS 1990 and 1995 data over Cuprite, Nevada. Solar zenith angles and atmospheric conditions are those experienced during the overflights. The AVIRIS 1990 S/N profile was derived from the standard deviation of a hundred pixel average reflectance spectrum of AVIRIS data over the Alkali Flat playa 6 km south of Cuprite. The AVIRIS 1995 S/N profile was derived from the standard deviation of the dark measured at the end of the flight line corrected to reflectance using the method outlined by Boardman (1995).

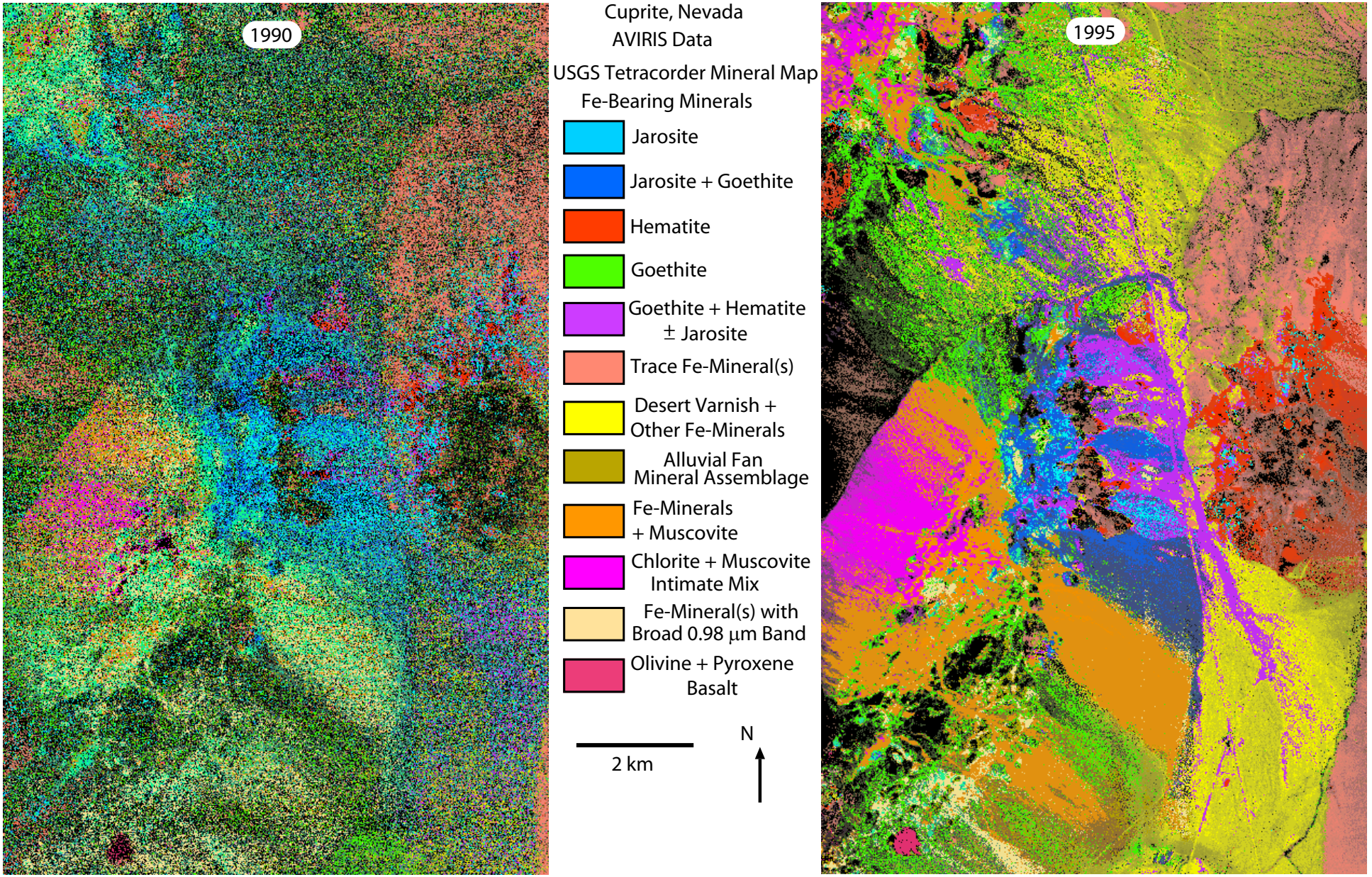

Figure 23. Mineral map of the electronic absorption spectral region (0.4 -1.35μm) created using the Tetracorder algorithm from AVIRIS data collected in July 1990 and June 1995 over the hydrothermal alteration systems at Cuprite, Nevada. The signal-to-noise ratio of the 1995 data is about four times higher than that of the 1990 data in this spectral region. Neither image is geometrically registered to avoid resampling of pixels which could modify the pattern of noise, consequently they approximately cover the same area on the ground.

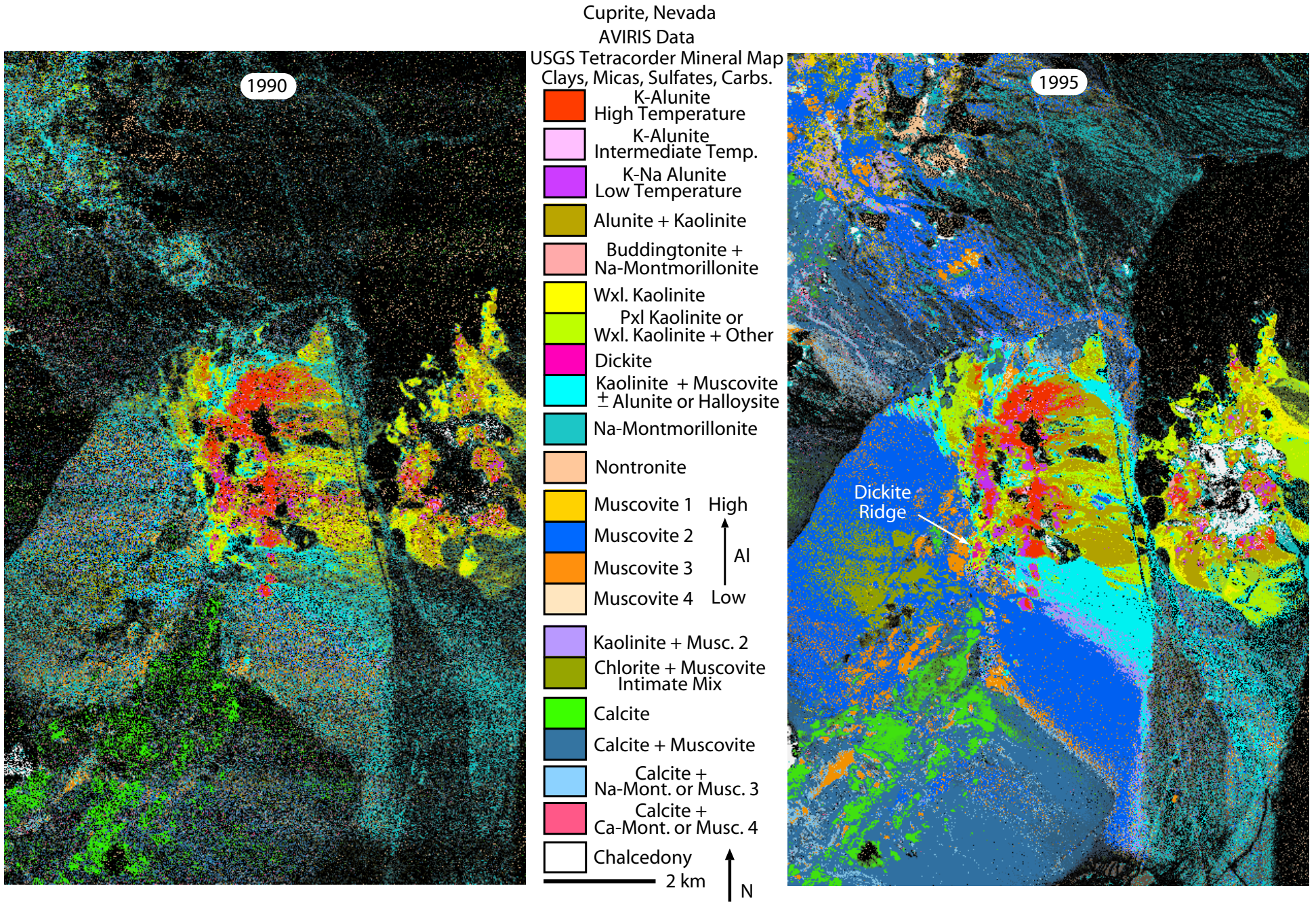

Figure 24. Mineral map of the vibrational absorption spectral region (1.35 - 2.5μm) created using the Tetracorder algorithm from AVIRIS data collected over Cuprite. The signal-to-noise ratio of the 1995 data is about six times higher than that of the 1990 data in this spectral region. The 1990 map has mineral patterns with noise levels similar to that of the 50% correct level example shown in Figure 12, whereas the level of mineral pattern noise in the 1995 mineral map resembles that at the 90% correct level. Coherent mineral patterns in the 1995 data can be used to make geologic interpretations that would be only marginally possible with the 1990 data. As in the previous figure, neither image is geometrically registered. Carb. = carbonate; temp. = temperature; wxl. = well-crystallized; pxl. = poorly-crystallized; musc. = muscovite; mont. = montmorillonite.

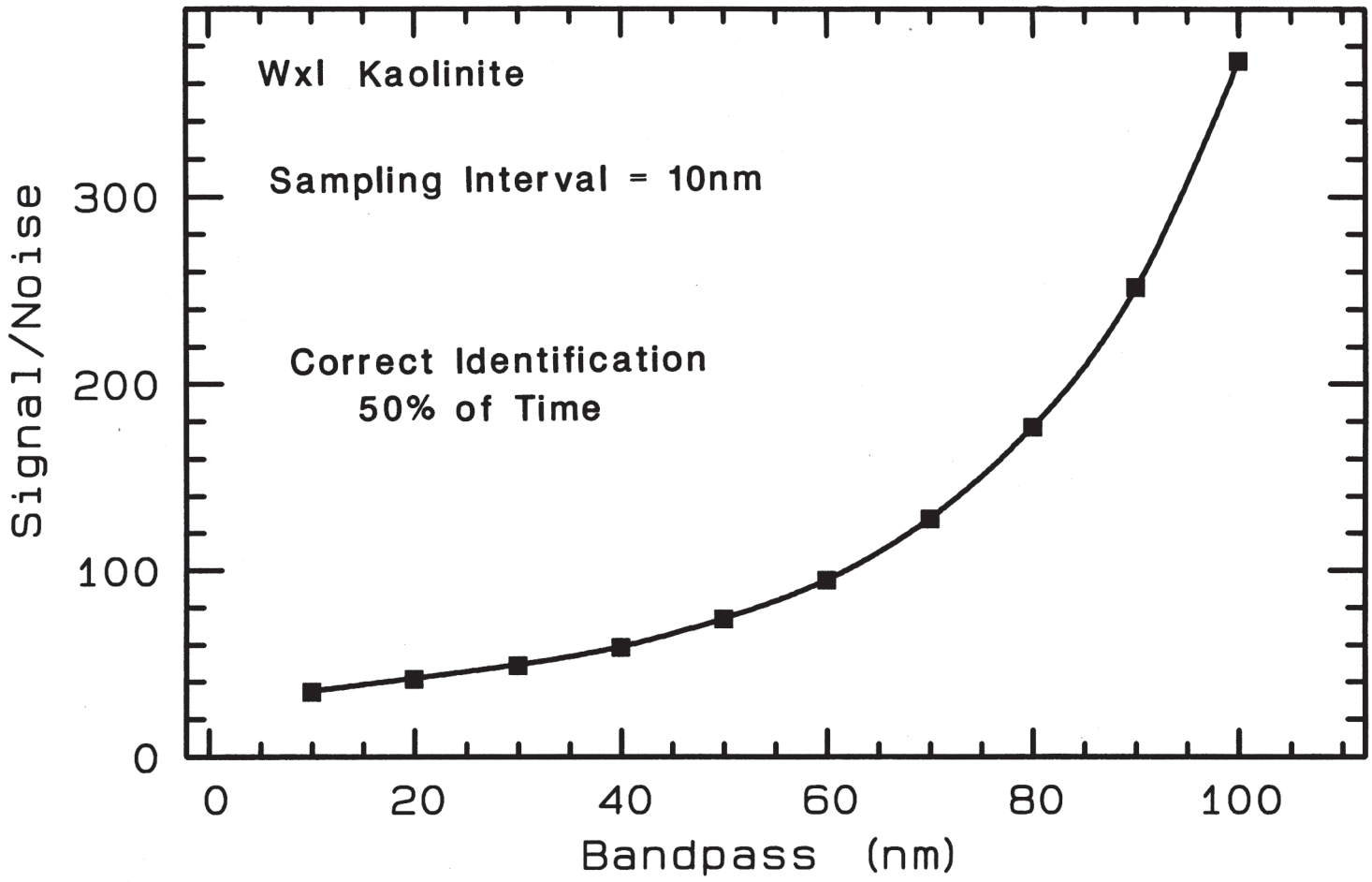

Figure 25. Signal-to-noise of identification (S/N_{ID}) curve showing S/N_{ID} values for the 50% correct level as a function of bandpass for well-crystallized kaolinite. The sampling interval of the test spectra was held constant at 10 nm. Signal-to-noise of identification increases rapidly at broad bandpasses, indicating that as bandpass exceeds the absorption band's FWHM confusion with spectral features of other materials may prevail.

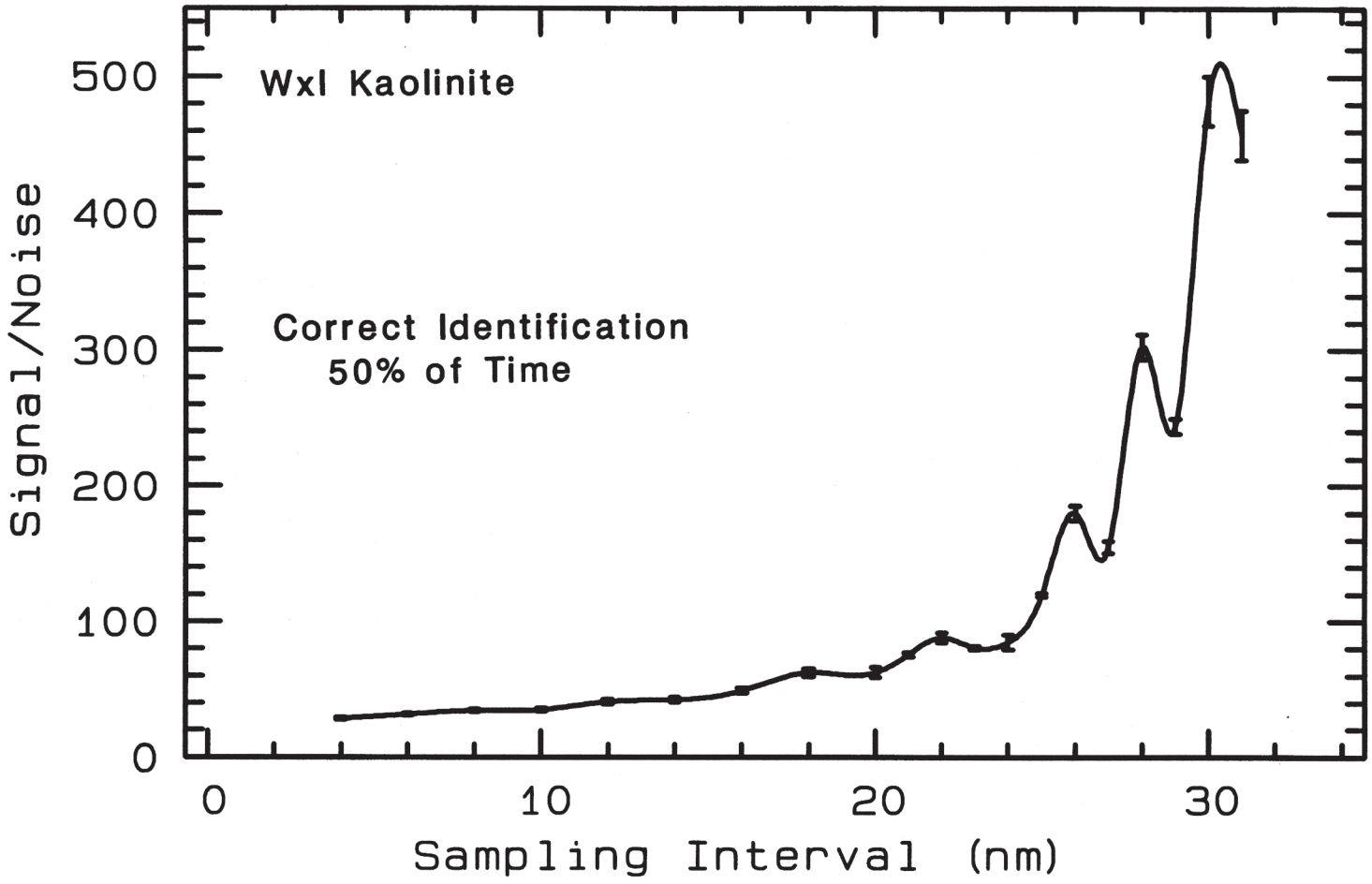

Figure 26. Signal-to-noise of identification (S/N_{ID}) curve showing S/N_{ID} values for the 50% correct level as a function of sampling interval for well-crystallized kaolinite. Test spectra are critically sampled (bandpass = sampling interval). Bars represent estimates of error in the position of identity curves used to derive the S/N_{ID} values.

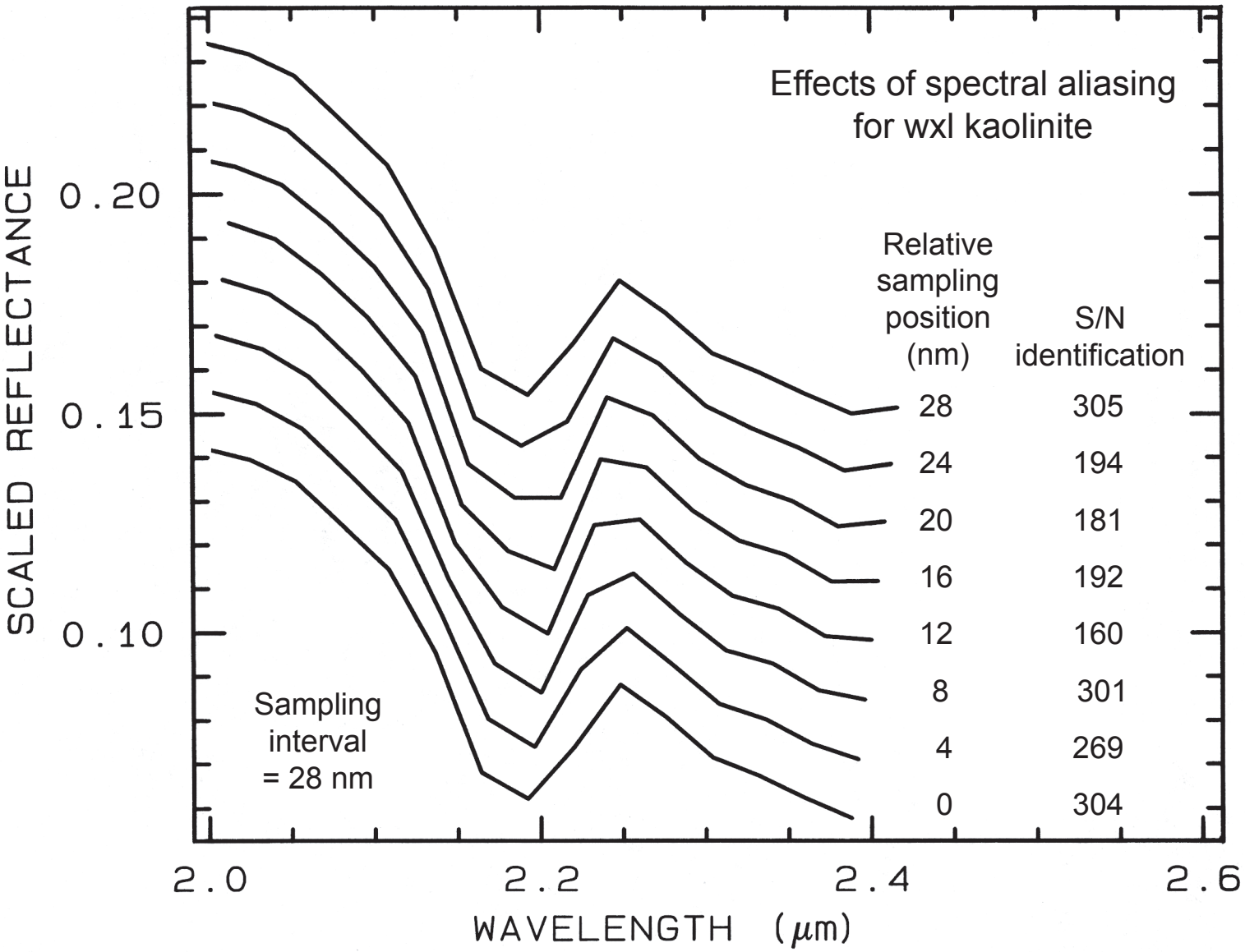

Figure 27. Details of the 2.2-μm absorption of a well-crystallized kaolinite convolved eight times to a bandpass and sampling interval equal to 28 nm, each time shifting the sampling position 4 nm toward shorter wavelengths. Listed to the right of the spectra are the corresponding signal-to-noise of identification values for the 50% correct level calculated for noisy test spectra generated from each convolved kaolinite spectrum.

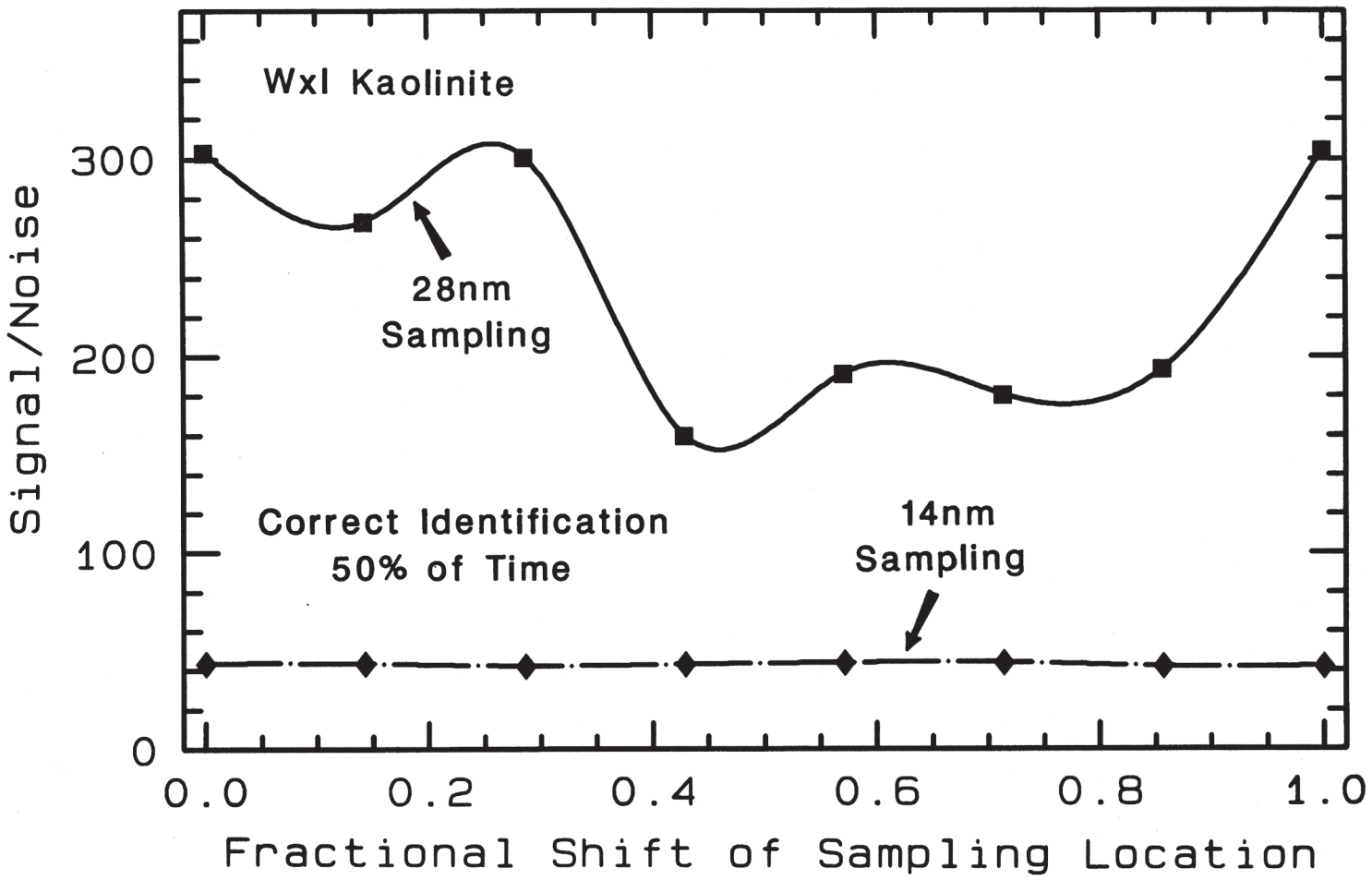

Figure 28. Signal-to-noise of identification values at the 50% correct level for noisy well-crystallized kaolinite test spectra convolved to 28 and 14 nm sampling intervals as a function of fractional shift of the sampling position. Upper curve sampling positions were shifted 4 nm for each successive set of noisy test spectra; bottom curve sampling positions were shifted 2nm. Note that "ringing" is almost non-existent in the lower curve.

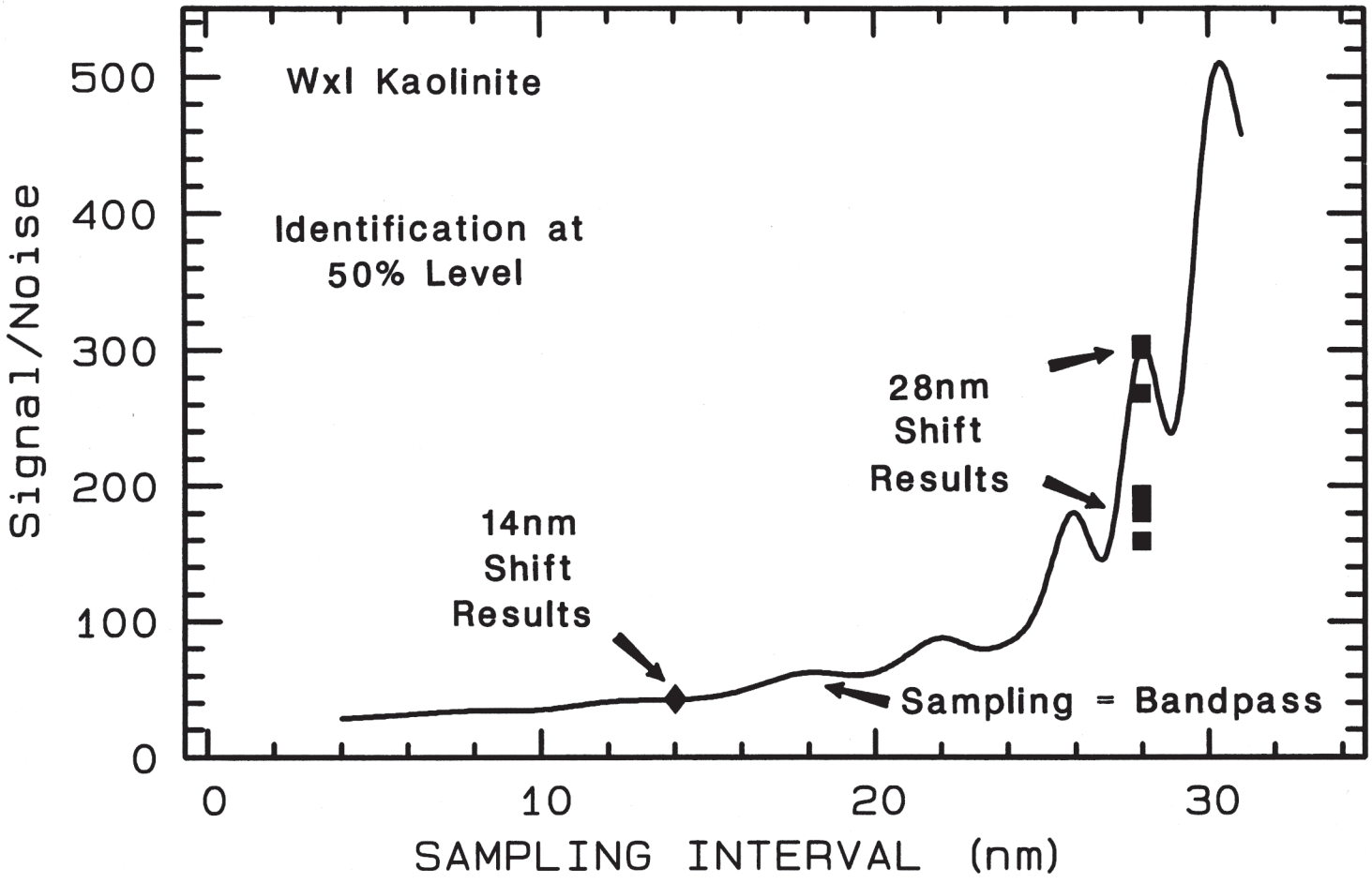

Figure 29. Signal-to-noise of identification values at the 50% correct level ($S/N_{ID50\%}$) from Figure 28 plotted on the well-crystallized kaolinite $S/N_{ID50\%}$ curve from Figure 26. Note that S/N_{ID} values of the14 nm spectra completely overlap and that the separation between S/N_{ID} values of the 28 nm spectra has the same amplitude as "ringing" in the S/N_{ID} curve.

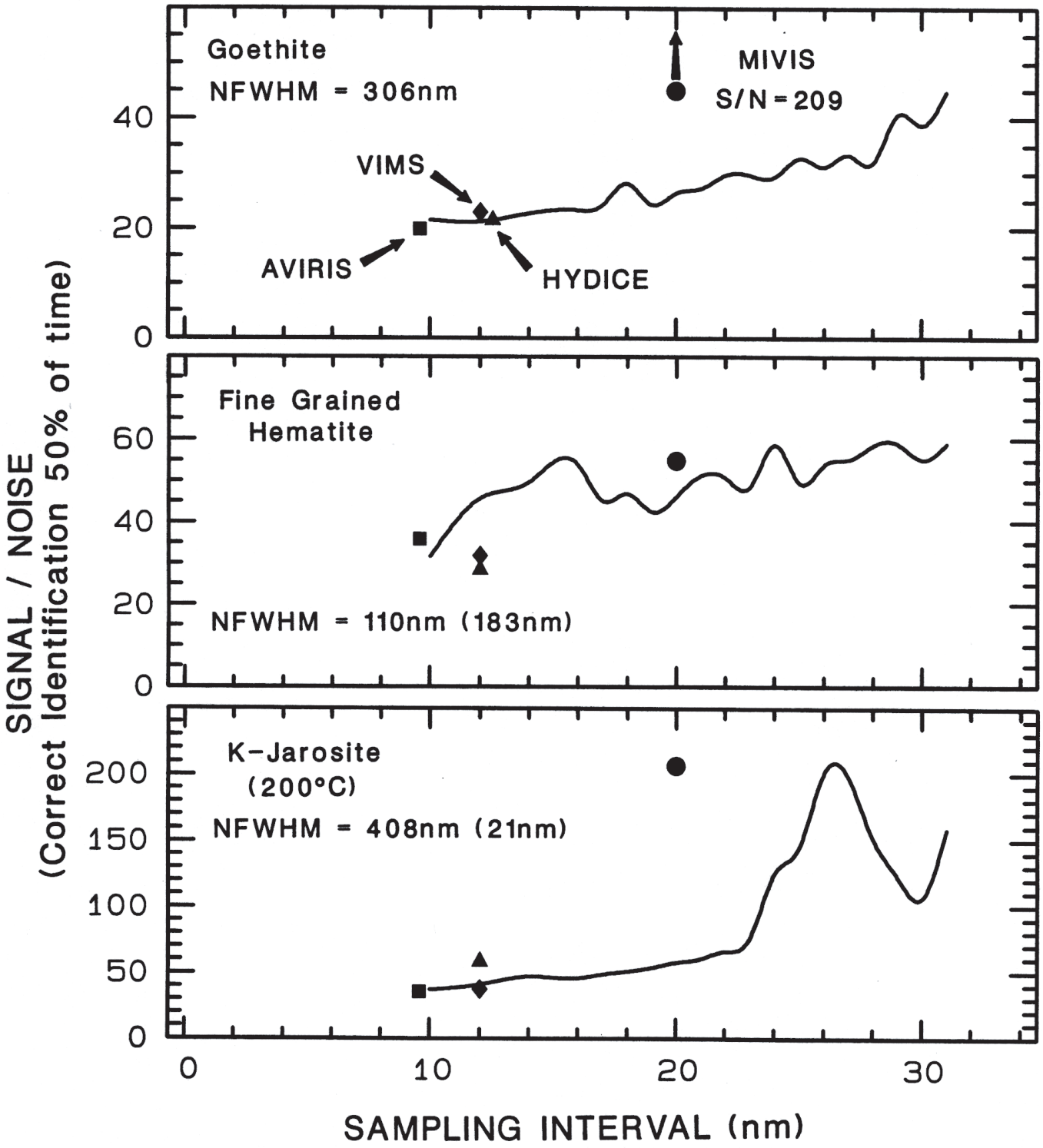

Figure 30. Signal-to-noise of identification curves at the 50% correct level ($S/N_{ID50\%}$) for minerals with absorptions in the electronic region. Test spectra were critically sampled. For each mineral, NFWHM is the natural full width half maximum of each absorption band measured from spectra collected at high spectral resolution. Numbers in parentheses are the NFWHM values of subordinate absorption bands. Symbols represent $S/N_{ID50\%}$ values for each imaging spectrometer. HYDICE and VIMS S/N_{ID} values plot below the hematite S/N_{ID} curve because of variations in the sampling intervals of these instruments which change over the wavelength range of the diagnostic hematite absorptions. MIVIS S/N_{ID} values plot above the S/N_{ID} curves for goethite, hematite, and K-jarosite because only the 0.48-µm absorption in each of these phases can be used for identification due to the 0.83 to 1.15 µm gap in MIVIS spectral coverage.

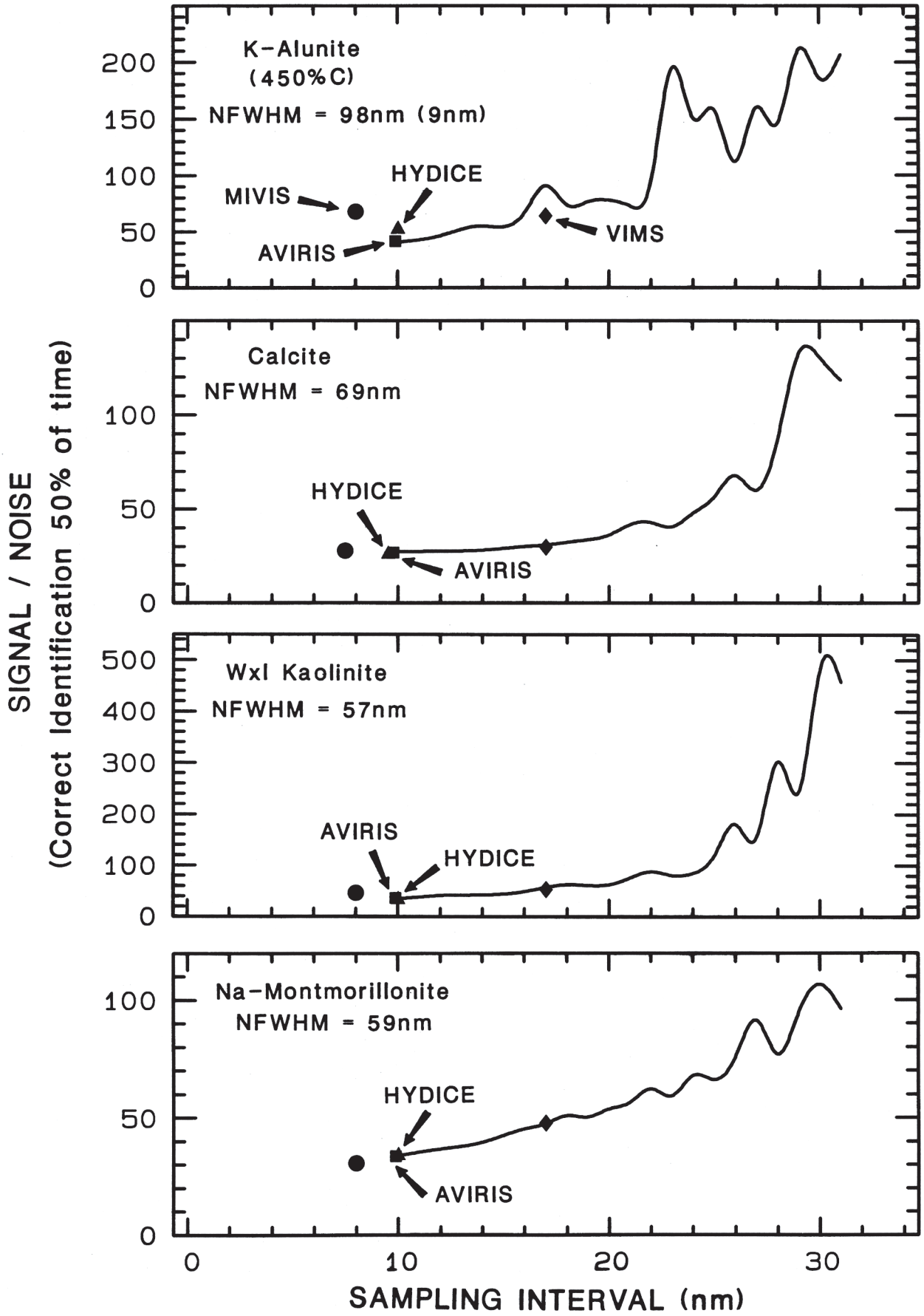

Figure 31. Signal-to-noise of identification curves at the 50% correct level ($S/N_{ID50\%}$) for minerals with absorptions in the vibrational region. Test spectra were critically sampled. See caption of Figure 30 for more details. For alunite the MIVIS S/N_{ID} value plots above the S/N_{ID} curve because this instrument's bandpass and sampling interval are too broad in the near-infrared to detect the diagnostic 1.48-μm alunite absorption.

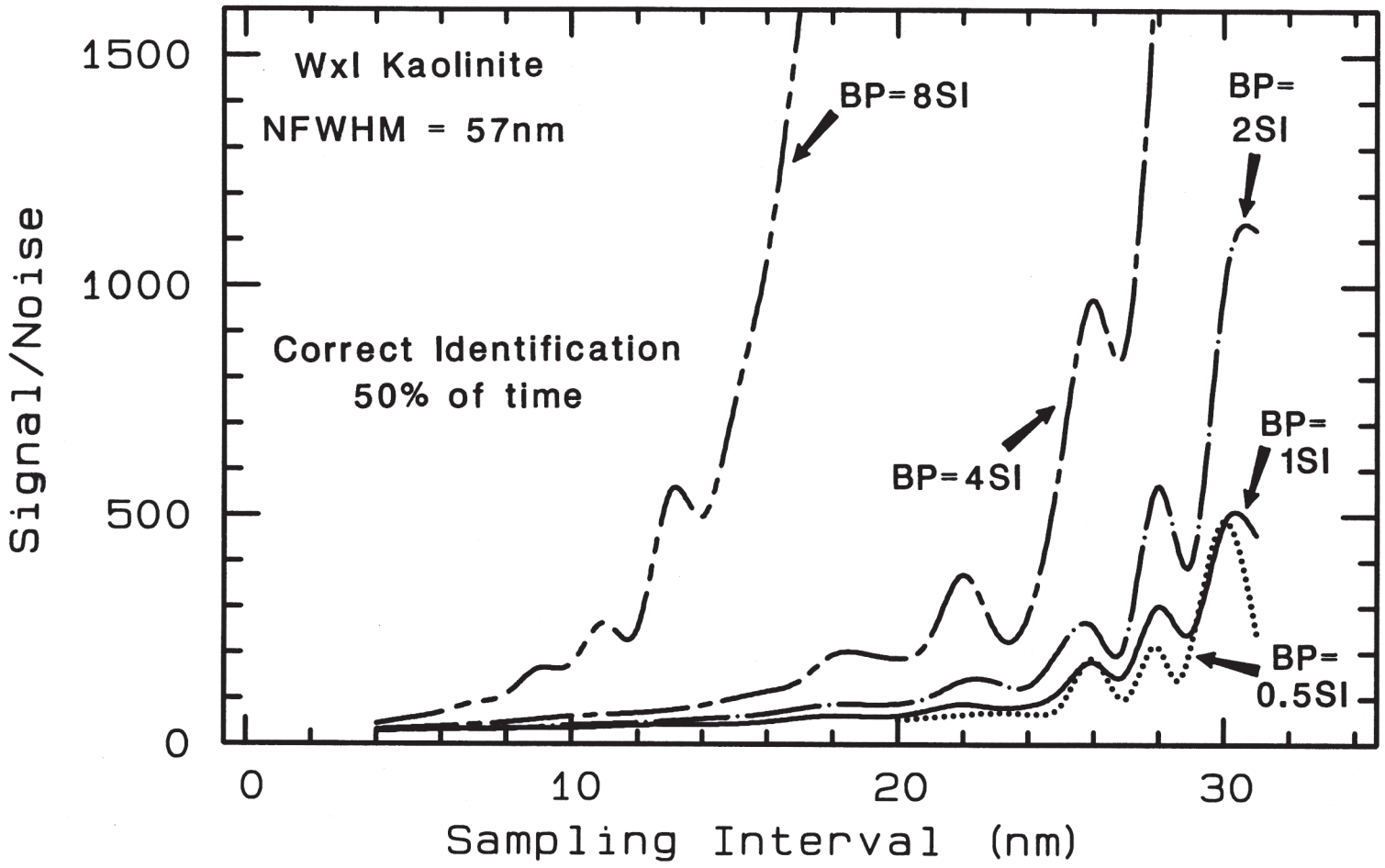

Figure 32. Signal-to-noise of identification (S/N_{ID}) curves for well-crystallized kaolinite for bandpasses 0.5, 1 (critical sampling), 2 (Nyquist sampling), 4, and 8 times the sampling interval at the 50% correct level. Note that the base of the identification walls shift to narrower sampling intervals and ringing intensifies as bandpass broadens. Overlap between the dotted curve (which begins at 20 nm) and the solid curve is likely caused by spectral aliasing in the undersampled spectra used to calculate S/N_{ID} values of the dotted curve.

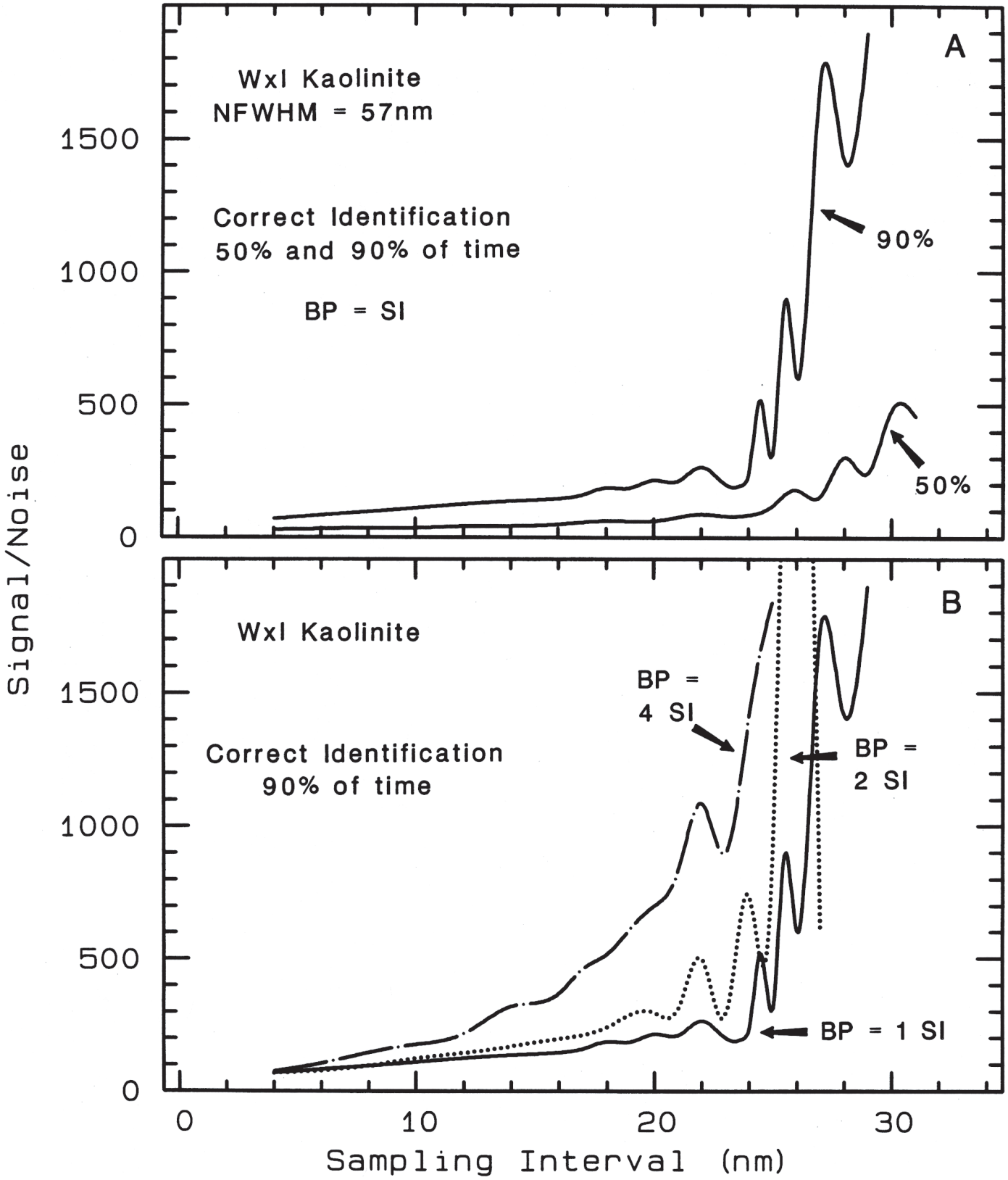

Figure 33. A) Signal-to-noise of identification curves for the 50% and 90% correct levels for well-crystallized kaolinite. Test spectra were critically sampled. B) Signal-to-noise of identification curves (S/N_{ID}) at the 90% correct level for well-crystallized kaolinite using test spectra with bandpasses equal to 1, 2, and 4 times the sampling interval (SI). Note that the curves are vertically separated at narrow bandpass (BP) and SI values and that the amplitude of "ringing" at 26 nm is greater than the overall height of the identification wall for the BP = 2 SI curve. On the BP = 2 SI curve, a 1 nm broadening of the SI increases the S/N_{ID} by an order of magnitude where $S/N_{ID} = 720$ at 25 nm and $S/N_{ID} > 7200$ at 26 nm.

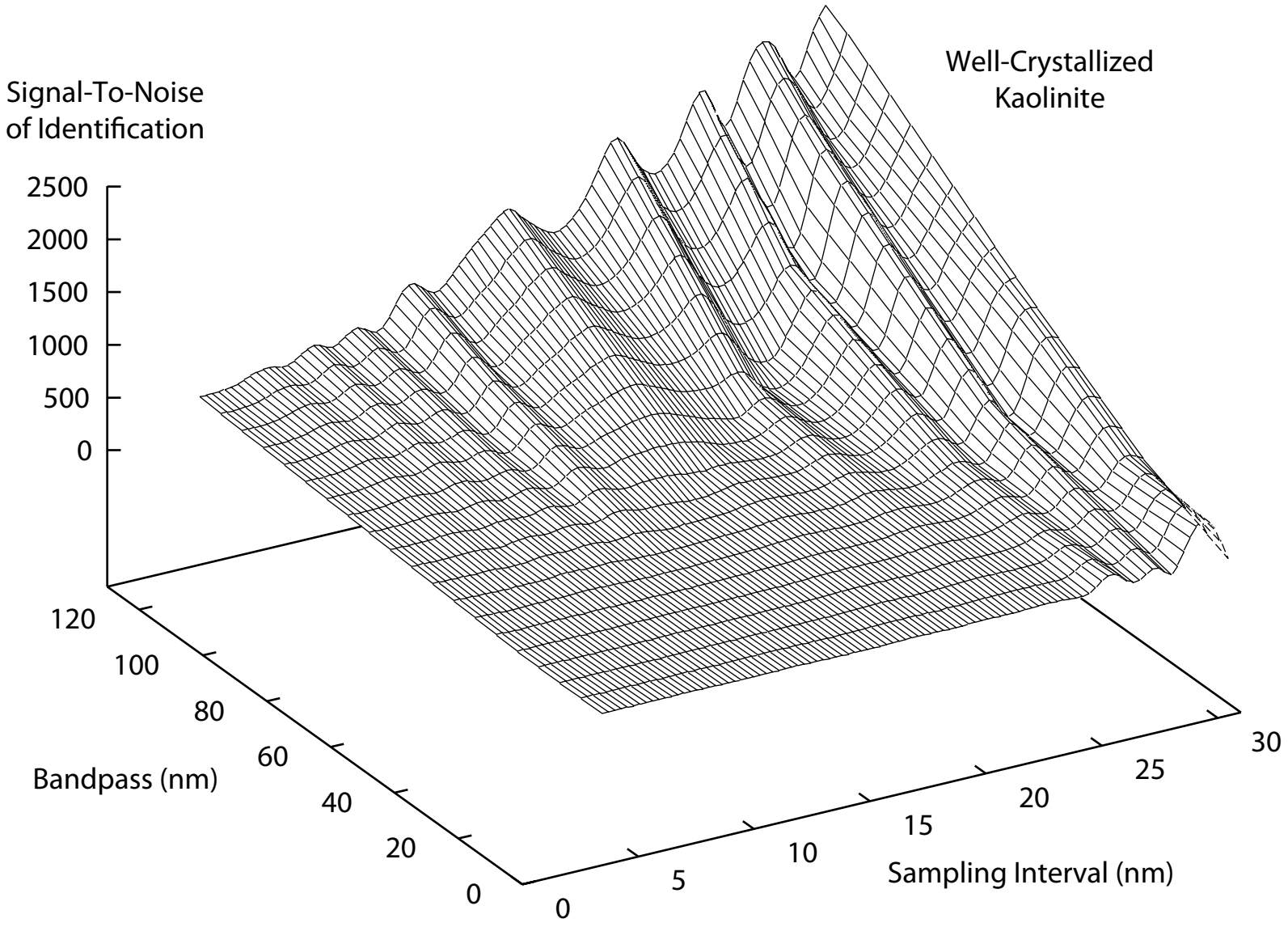

Figure 34. Signal-to-noise of identificationsurface for well-crystallized kaolinite at the 50% correct level as a function of bandpass and sampling interval. Test spectra were critically sampled.

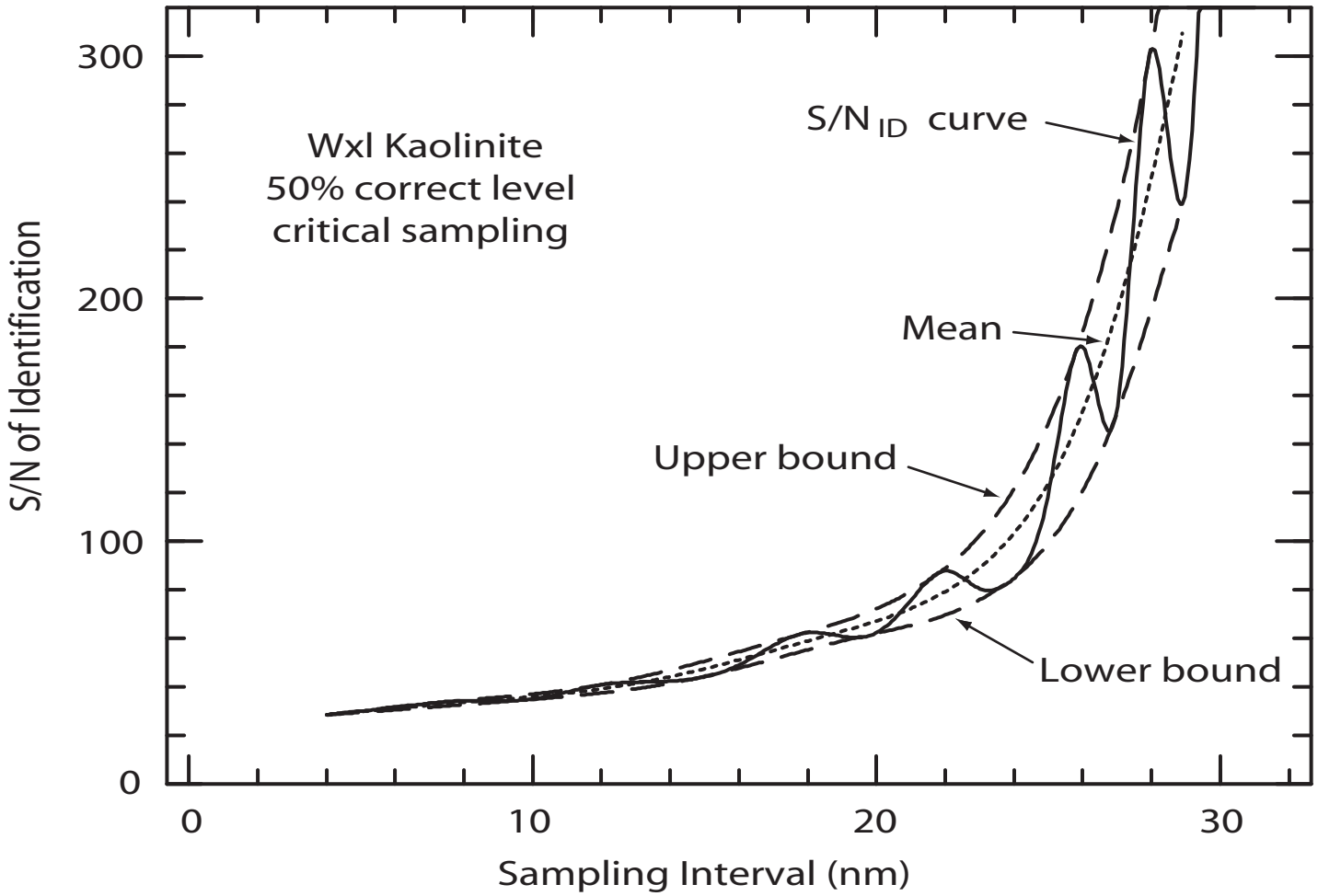

Figure 35. Signal-to-noise of identification (S/N_{ID}) curve for well-crystallized kaolinite at the 50% correct level and critical sampling bounded by upper and lower curves (dashed) drawn tangential to the oscillations caused by spectral aliasing. Because the locations of peaks and troughs on the S/N_{ID} curve depend on the wavelengths at which the kaolinite spectra were sampled (e.g., as demonstrated in Figures 24 to 26) the bounding curves theoretically encompass all possible values of the S/N required for identification. The mean S/N_{ID} curve (dotted) can be estimated by taking the average of the upper and lower bounding curves.

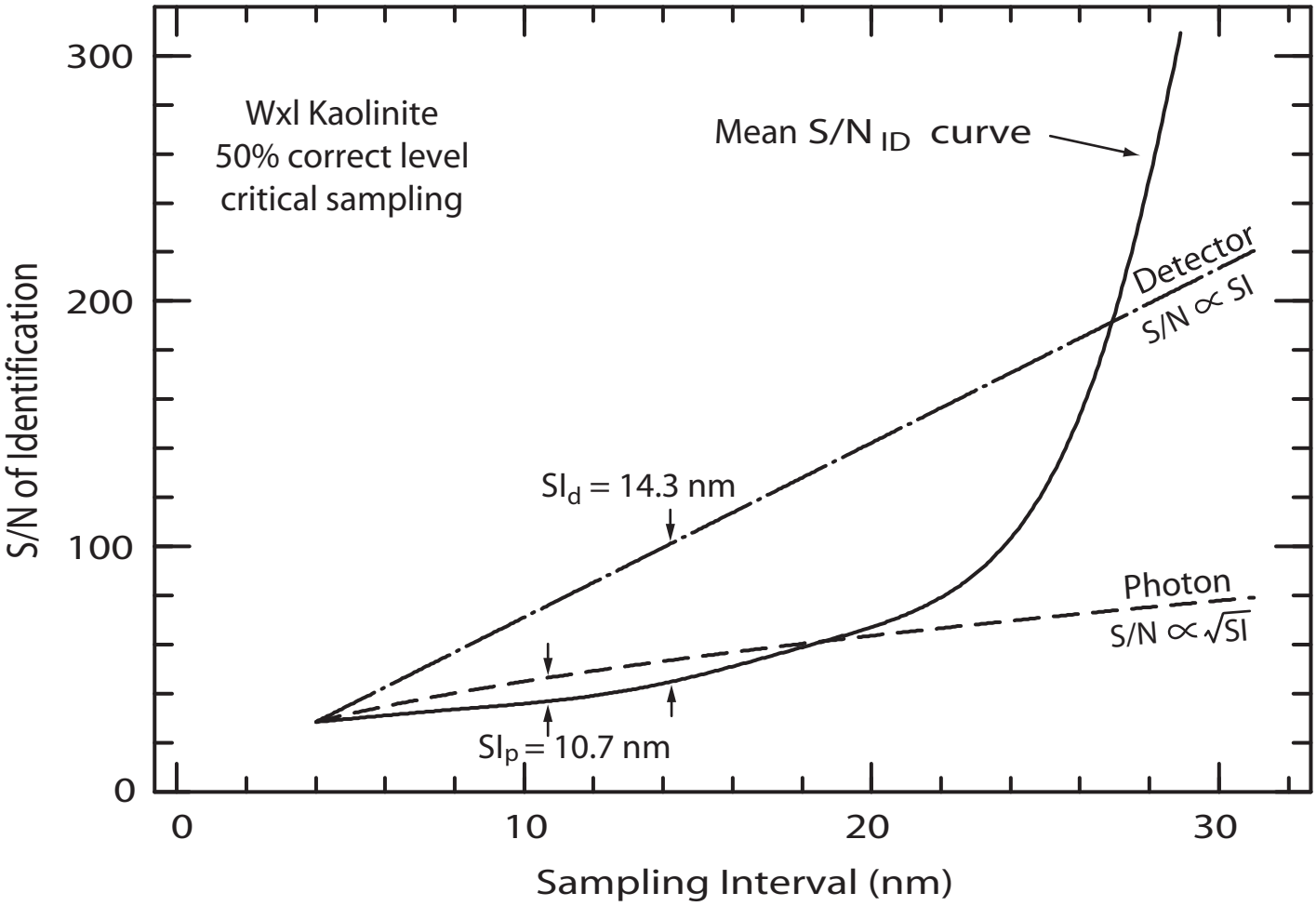

Figure 36. Dividing the achievable signal-to-noise ratio (S/N) curves for a photon-noise-limited system (dashed curve) and a detector-noise-limited system (dash - dotted curve) by the mean signal-to-noise of identification (S/N_{ID}) curve for well-crystallized kaolinite at the 50% correct level results in curves whose maximum values are the optimum sampling interval (SI) values for photon (SI_p) and detector (SI_d) noise limited systems. The S/N is proportional to the $\sqrt{SI}$ in a photon-noise-limited system and directly proportional to the SI in a detector-noise-limited system. The positions of the photon and detector achievable curves are not absolute. The S/N in a photon-noise-limited system is always greater than in a detector-noise-limited system.

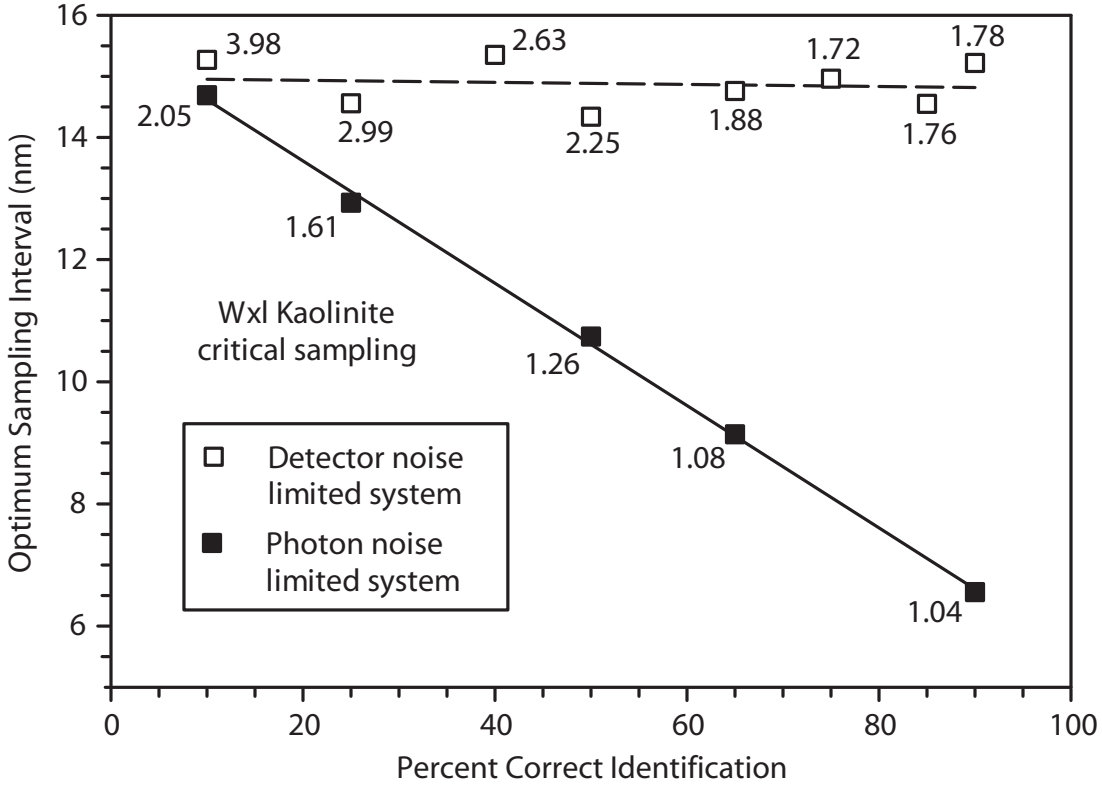

Figure 37. Optimum sampling interval (SI) values for both photon(SI_p) and detector (SI_d) noise limited systems as a function of percent correct identification for well-crystallized kaolinite determined using the technique shown in Figure 36. The solid line is best fit to the photon-noise-limited data described by: optimum SI_p = ((% correct * -0.1001) + 15.62) with $r^2 = 0.998$. The dashed line is best fit to the detector-noise-limited data described by: optimum SI_d = ((% correct * -0.001707) + 14.97) with $r^2 = 0.017$. This low r^2 value shows that the optimum sampling interval for the detector case is relatively independent of the percent correct identification level. Greater scatter in the detector-noise-limited data is due to the relatively larger magnitude of spectral alias ringing at higher SI values resulting in greater uncertainty in estimates of the mean signal-to-noise of identificationcurve. Numbers by each symbol indicate the ratio of achievable / require S/N.

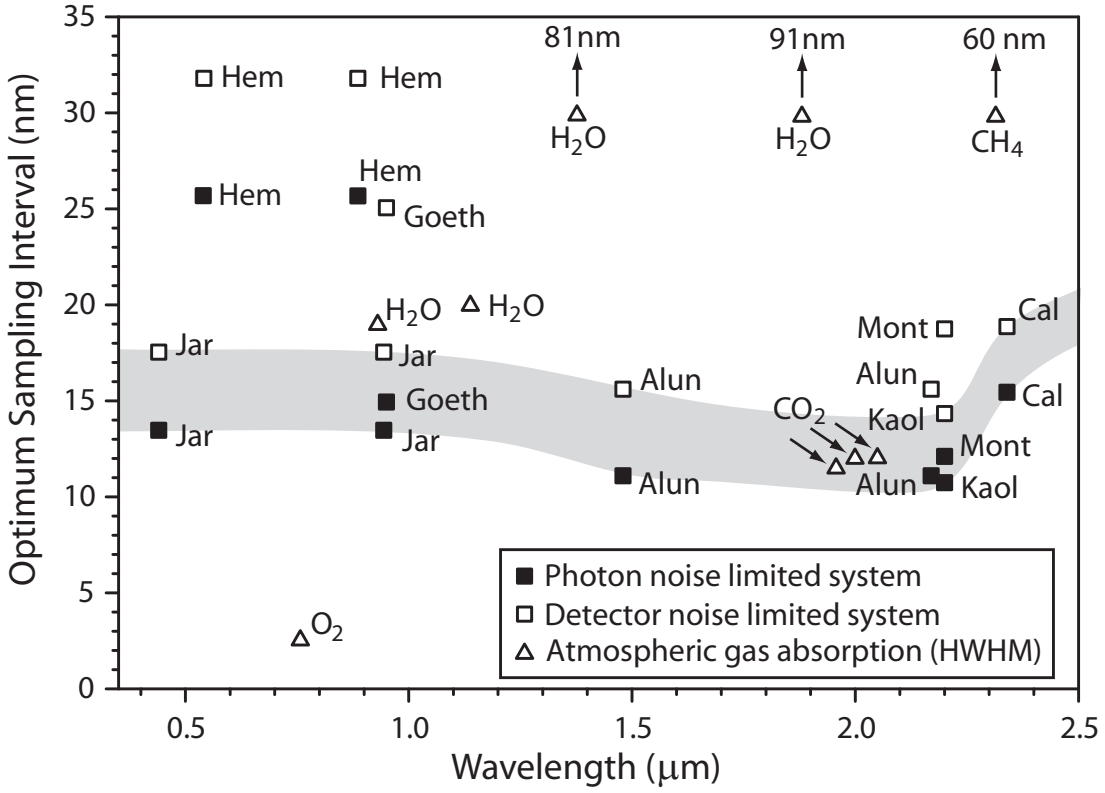

Figure 38. Optimum sampling interval (SI) values for photon- and detector-noise-limited systems at the 50% correct identification level versus wavelength positions for the diagnostic spectral absorptions used for identification of seven alteration minerals. The gray zone's lower boundary is the minimum optimal SI for identification of the minerals as a function of wavelength for a photon-noise-limited system. The gray zone's upper boundary is the minimum optimal SI for a detector-noise-limited system. Triangles mark wavelength positions and Half-Width-Half-Maxima (HWHM) of terrestrial atmospheric gas absorptions; the locations of the triangles do not necessarily depict the optimum SI values for identification of these gases. Arrows above H_2O and CH_4 triangles indicate that the HWHM values of absorptions from these gases at these wavelengths are beyond the upper bound of the plot at the specified SI values. Jar = jarosite; Hem = hematite; Goeth = goethite; Alun = K-alunite; Kaol = well-crystallized kaolinite; Mont = Na-montmorillonite; Cal = calcite.